

PAPER

Infrared and reflectron time-of-flight mass spectroscopic study on the synthesis of glycolaldehyde in methanol (CH₃OH) and methanol–carbon monoxide (CH₃OH–CO) ices exposed to ionization radiation†

Surajit Maity, Ralf I. Kaiser* and Brant M. Jones*

Received 6th December 2013, Accepted 6th February 2014

DOI: 10.1039/c3fd00121k

We present conclusive evidence on the formation of glycolaldehyde (HOCH₂CHO) synthesized within astrophysically relevant ices of methanol (CH₃OH) and methanol–carbon monoxide (CH₃OH–CO) upon exposure to ionizing radiation at 5.5 K. The radiation induced chemical processes of the ices were monitored on line and *in situ* via infrared spectroscopy which was complimented by temperature programmed desorption studies post irradiation, utilizing highly sensitive reflectron time-of-flight mass spectrometry coupled with single photon fragment free photoionization (ReTOF-PI) at 10.49 eV. Specifically, glycolaldehyde was observed *via* the ν_{14} band and further enhanced with the associated frequency shifts of the carbonyl stretching mode observed in irradiated isotopologue ice mixtures. Furthermore, experiments conducted with mixed isotopic ices of methanol–carbon monoxide (¹³CH₃OH–CO, CH₃¹⁸OH–CO, CD₃OD–¹³CO and CH₃OH–C¹⁸O) provide solid evidence of at least three competing reaction pathways involved in the formation of glycolaldehyde *via* non-equilibrium chemistry, which were identified as follows: (i) radical–radical recombination of HCO and CH₂OH formed *via* decomposition of methanol – the “two methanol pathway”; (ii) *via* the reaction of one methanol unit (CH₂OH from the decomposition of CH₃OH) with one carbon monoxide unit (HCO from the hydrogenation of CO) – the “one methanol, one carbon monoxide pathway”; and (iii) formation *via* hydrogenation of carbon monoxide resulting in radicals of HCO and CH₂OH – the “two carbon monoxide pathway”. In addition, temperature programmed desorption studies revealed an increase in the amount of glycolaldehyde formed, suggesting further thermal chemistry of trapped radicals within the ice matrix. Sublimation of glycolaldehyde during the warm up was also monitored *via* ReTOF-PI and validated *via* the mutual agreement of the associated isotopic frequency shifts within the infrared band positions and the identical sublimation profiles obtained from the ReTOF spectra and infrared spectroscopy of the

Department of Chemistry, W. M. Keck Research Laboratory in Astrochemistry, University of Hawaii at Manoa, Honolulu, Hawaii, HI, 96822, USA. E-mail: ralfk@hawaii.edu; brantmj@hawaii.edu

† Electronic supplementary information (ESI) available. See DOI: 10.1039/c3fd00121k

corresponding isotopes. In addition, an isomer of glycolaldehyde (ethene-1,2-diol) was tentatively assigned. Confirmation of the identified pathways based on infrared spectroscopy was also obtained from the observed ion signals corresponding to isotopomers of glycolaldehyde. These coupled techniques provide clear, concise evidence of the formation of a complex and astrobiologically important organic, glycolaldehyde, relevant to the icy mantles observed in the interstellar medium.

1. Introduction

During the last decade, the glycolaldehyde molecule (HCOCH_2OH) has received considerable attention in the astronomy, astrochemistry, and astrobiology communities. Glycolaldehyde was first detected in the richest molecular source in the Galaxy, Sgr B2(N),¹ located in the galactic center molecular cloud Sagittarius B2, also known as the Large Molecular Heimat.² Chemical differentiation was later observed in the structural isomers of glycolaldehyde,³ *i.e.* methyl formate (HCOOCH_3) and acetic acid (CH_3COOH), whose formation routes are unknown.² Consequently, an understanding of the chemistry behind the formation of glycolaldehyde and its isomers may help to explain the observed differentiation, since structural isomers can be exploited as a chemical clock to unravel the underlying chemistry in extraterrestrial environments such as star forming regions. A subsequent extensive line search of glycolaldehyde allowed the determination of the fractional abundance of $f(\text{H}_2) \approx 5.9 \times 10^{-11}$ in Sgr B2 (N).⁴ From here, a tentative identification of glycolaldehyde outside of the galactic center was made in 2005 towards the hot core G31.40+0.31,⁵ and later confirmed by the same authors in 2009,⁶ with the glycolaldehyde emission originating from the hottest (≥ 300 K) section with a rather large (estimated) fractional abundance of $f(\text{H}_2) \approx 5 \times 10^{-8}$. This yielded the only confirmed detection outside our galaxy. In addition to glycolaldehyde, other complex organic molecules (COM) have been detected in the galactic center, such as methyl formate (HCOOCH_3), acetaldehyde (CH_3COH), ketene (H_2CCO), and ethylene oxide ($\text{c-C}_2\text{H}_4\text{O}$).⁷ The most recent detection of glycolaldehyde has been with the Atacama Large Millimeter Array (ALMA) toward the protostellar binary system IRAS 16293-2422.⁸ Here, glycolaldehyde was found in the warm (200–300 K) gas close to the individual components of the binary, with an estimated fractional abundance of $f(\text{H}_2) \approx 5 \times 10^{-9}$, which the authors note correlates with an origin related to the energetic processing *via* UV photolysis of an icy grain mantle consisting of methanol and carbon dioxide followed by sublimation during the warm up phase.

As glycolaldehyde is the simplest monosaccharide sugar detected in numerous astrophysical environments ranging from hot cores to the galactic center molecular cloud, the detection of glycolaldehyde immediately prompted interest within the astrobiological community, as the presence of glycolaldehyde directly pertains to the 'origin of life' question. Here, glycolaldehyde is one of the key precursors in the formation of ribonucleic acid (RNA).^{9–13} Since the 'RNA World' origin of life hypothesis^{14–17} is currently one of the dominating theories within the community,^{18,19} glycolaldehyde has been heavily implicated in the literature on the premise that it correlates well with the abiotic formation of ribose, which is a central back bone of RNA. Yet, one of the main difficulties in considering an 'RNA World' relationship to the origin of life is the complication of forming RNA

prebiotically.^{20,21} There has been experimental evidence however, showing that abiotic formation of nucleotides from basic starting materials is possible, and thus not an entirely impractical chemical route. In particular, glycolaldehyde can react *via* an aldol condensation to ultimately produce ribose.²² Additionally the polymerization of formaldehyde (the formose reaction²³) has been suggested as plausible prebiotic route to glycolaldehyde and ribose (Shapiro, 2000).²⁴ However, as pointed out by Shapiro (2000),²⁴ no prebiotic route exists that preferentially leads to the synthesis of ribose specifically over a conglomerate of other sugars, despite many efforts. Some success has been demonstrated in generating ribose 2,4-diphosphate in a possibly prebiotic reaction of monophosphate glycolaldehyde and formaldehyde.²⁵ Also, it should be noted that ribose has been shown to be produced in elevated yields following a formose type mechanism in mixtures containing aldehyde, glycolaldehyde, and minerals such as pyrite, borate and silicates.²⁶ In addition, ribonucleotides were abiotically synthesized in a multistep reaction utilizing only cyanamide (CN₂H₂), cyanoacetylene (C₃HN), glyceraldehyde (C₃H₆O₃) and glycolaldehyde (HOCH₂CHO).²⁷ Consequently, the abiotic synthesis of nucleotides is feasible. Furthermore, as pointed out recently, an upper limit of 10⁸ kg year⁻¹ of glycolaldehyde may have been deposited on an early Earth *via* comets and interplanetary dust, in addition to the 10⁸ kg year⁻¹ that may have been formed *in situ* on an early Earth.²⁸ Additionally, the detection of glycolaldehyde around the newly formed star IRAS 16293B implies that this molecule may be involved in planet forming processes.⁸

Due to the importance of glycolaldehyde, over the last few decades, studies exploring the radiation induced synthesis of glycolaldehyde pertaining to ices of methanol have been numerous. Of the first papers, most were focused on spectroscopy of radicals; the photolysis ($E_{hv} = 145$ nm, 8.4 eV) of methanol isolated in an argon matrix produced the hydroxymethyl (CH₂OH) radical.²⁹ The production of this CH₂OH radical in addition to the methyl (CH₃) and the methoxy radical (CH₃O) *via* X-ray radiolysis of crystalline methanol was later confirmed using electron pair resonance spectroscopy at 4.2 K.³⁰ Products of γ -irradiated methanol ice were found to be molecular hydrogen (H₂), ethylene glycol (HOCH₂CH₂OH), methane (CH₄), carbon monoxide (CO), dimethyl ether (CH₃OCH₃), and ethanol (CH₃CH₂OH).³¹ From here, pure methanol and binary mixtures of methanol with water and carbon monoxide were exposed to distinct sources of ionizing radiation (summarized in Table S1 of the ESI[†]). All of the previous experimental results predominantly agree that simple molecules (CO, CO₂, CH₄, H₂CO), with some degree of overlapping with the detection of ethanol, ethylene glycol, water, and the formyl radical (HCO), are formed *in situ via* energetic processing. Crucial discrepancies do exist however, such as the assignment of acetone, which was first suggested as a result of 3 keV He⁺ bombardment of pure methanol,³² and was subsequently tentatively assigned in later studies.^{33–36} However, the assignment of acetone was refuted in a study with 0.8 MeV H⁺ bombardment of a methanol–water mixture;³⁷ from this study, the assignment of the observed vibrational bands that were ascribed to acetone were subsequently attributed to the HCOO⁻ ion. Far IR spectroscopy was used to examine the phase change of crystalline to amorphous methanol induced by 0.7 MeV H⁺ irradiation. Although no products were specifically identified, the authors noted that the irradiated methanol would not re-crystallize with thermal annealing, which was attributed to additional products synthesized within the methanol ice matrix.³⁸ Higher order alcohols

were attributed to an unidentified feature at 1088 cm^{-1} after broad band UV photolysis of pure methanol ice *via* a hydrogen microwave discharge lamp at 10 K in addition to the standard group of daughter molecules (CO, CO₂, CH₄, H₂CO). This assignment of a higher mass alcohol was further verified by the observation that the IR band started to disappear (indicating sublimation) at 120 K and was completely gone at 230 K, suggesting a molecule with a similar volatility to methanol.³⁹ After the first detection of glycolaldehyde in the galactic center,¹ a resurgence in methanol irradiation experiments occurred in the hopes of explaining the origin of this sugar, along with its isomers, methyl formate and acetic acid. One of the first irradiation experiments to identify glycolaldehyde as a product of methanol ice exposed to ionizing radiation utilized 5 keV electrons, thereby simulating the track of secondary electrons generated within the trajectory of galactic cosmic rays⁴⁰ and a binary mixture of methanol and carbon monoxide.⁴¹ Here, glycolaldehyde was identified in irradiated methanol ices at 10 K and also following warm up, whereas in the binary mixture (CH₃OH–CO), glycolaldehyde in conjunction with methyl formate was immediately identified *in situ* at 10 K with a total applied dose of 0.7 eV per 16 amu. In addition, glycolaldehyde and methyl formate were distinguished by utilizing temperature programmed desorption coupled with gas phase detection *via* a quadrupole mass spectrometer based on the unique fragmentation pattern (*e.g.* the methyl formate cation – HCOO⁺) at distinct sublimation temperatures. Following the studies of Bennett *et al.*,^{40,41} similar work was conducted utilizing broad band UV photons produced *via* a hydrogen microwave discharge lamp, in which glycolaldehyde was only inferred as a potential product after photolysis of CH₃OH and CH₃OH–CO ices. Recently, glycolaldehyde was only briefly mentioned as an endogenous product upon exposure to 200 keV protons at relatively high doses of 34 eV⁴² and 18 eV⁴³ per 16 amu. In the most recent experiment, Chen *et al.* reported the formation of glycolaldehyde in irradiated methanol ices utilizing soft X-rays with peak energies of 300 eV and 550 eV over a broad band spectrum (250–1200 eV)⁴⁴ following warm up, in agreement with the previous observation of Bennett *et al.*;⁴¹ methyl formate, acetic acid, formic acid and ethylene glycol were also reported. No mention of glycolaldehyde was made in the experiments involving various heavy cosmic ray analogs,⁴⁵ or in the irradiation of methanol at very low doses with soft X-rays.⁴⁶ To summarize, numerous experiments have been conducted over recent decades regarding the chemical modification of methanol ices upon exposure to ionizing radiation relevant to astrophysical conditions. Within these studies, a general consensus on the formation of small molecules, which can be detected easily *via* infrared spectroscopy (FTIR) (CO, CO₂, H₂CO, CH₄) and for the most part ethanol, ethylene glycol, and methyl formate, has been ascertained. However, the main difference thus far is the ambiguity in the assignment of glycolaldehyde in the majority of the processed ices.

In this study, we present compelling evidence from infrared spectral data correlated for the first time with temperature programmed desorption studies exploiting single photon ionization (10.49 eV) reflectron time-of-flight mass spectrometry (ReTOF) gas phase detection of glycolaldehyde synthesized in irradiated ices of CH₃OH and CH₃OH–CO along with selected isotopologues, exposed to doses of up to 6.5 eV per molecule relevant to the life time of an interstellar icy grain within a cold molecular cloud prior to the warm up (star formation) phase; at this point the grain begins to warm, causing radicals to diffuse and the

endogenous radiolytically synthesized molecules to sublimate into the gas phase, allowing for direct observation *via* radio astronomical observations.

2. Experimental

The experiments were carried out in a novel, contamination-free ultra-high vacuum (UHV) chamber at the W. M. Keck Research Laboratory in Astrochemistry (Fig. 1). The main chamber was evacuated down to a base pressure typically of a few 10^{-11} Torr using oil-free magnetically suspended turbomolecular pumps backed with dry scroll pumps. A cold finger assembled from oxygen free high conductivity copper (OFHC) was coupled to a UHV compatible closed-cycle helium refrigerator (Sumitomo Heavy Industries, RDK-415E). A polished silver mirror was then mounted to the cold finger insulated with 0.1 mm thick indium foil to ensure thermal conductivity, and subsequently cooled to a final temperature of 5.5 ± 0.1 K; the entire ensemble was freely rotatable within the horizontal center plane, and translatable in the vertical (*z*-axis) *via* a UHV compatible bellow (McAllister, BLT106) and differential pumped rotational feed through (Thermoionics Vacuum Products, RNN-600/FA/MCO). From here, the corresponding gases were then deposited through a glass capillary with a background (uncorrected for ion gauge sensitivity) pressure reading in the main chamber of 5×10^{-8} Torr for approximately 3 minutes, yielding an ice sample with final thicknesses of 510 ± 10 nm for pristine methanol ices, and 495 ± 10 nm for mixed ices of

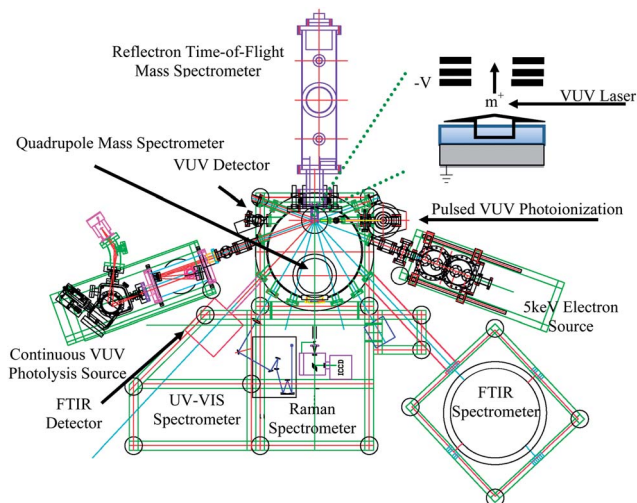


Fig. 1 Schematic top view of the main chamber including the analytical instruments, radiation sources, and the cryogenic target (point of converging lines). The alignment of the cryogenic target, radiation sources, infrared, Raman, and UV-vis spectrometer allows simultaneous online and *in situ* measurements of the modification of the targets upon the exposure to irradiation. After the irradiation, the cold head can be rotated 180° to face the ReTOF mass spectrometer; the target can then be warmed up allowing the newly formed products to sublimate, whereupon they are photoionized and mass analyzed. The inset (top right) shows the geometry of the ReTOF ion source lenses with respect to the target and ionization laser.

methanol-carbon monoxide. The thickness of the sample was determined *in situ* using laser interferometry. Here, the cooled silver target was rotated to face a HeNe laser (CVI Melles-Griot; 25-LHP-230, 632 nm), which struck the target at an incident angle of 4° relative to the sample normal, and was reflected towards a photodiode (CVI Melles-Griot Si Photodiode; 13DAS005 with a 632.8 nm narrow band pass filter, CVI XII-632.8-12.6M). The induced current in the photodiode was monitored as a function of time with a picoammeter (Keithley Model 6485), while the gas was introduced into the chamber at a constant rate through a precision leak valve, whereupon it finally condensed onto the low temperature silver target. During the deposition, the HeNe laser was reflected off the surface of the silver target and the freshly deposited ice sample, causing an interference pattern. The relation between the period of the interference curve between two maxima or minima relates to a change in thickness, Δd , as described by Heavens,⁴⁷ where λ_0 is the laser wavelength (632.8 nm), θ_i is the incident angle (4°), and n_f is the refractive index of the ice. Here, *a priori* knowledge of the index of refraction (n_f) is required for accurate determination of the deposited ice thickness. Taking into consideration the known index of refraction for the substrate,^{48–50} the index of refraction can also be derived by measuring the intensity ratio between the maximum and minimum of the measured interference curve.^{49,50} From this technique, we derived an index of refraction $n_f = 1.34 \pm 0.02$ for pure methanol, in agreement with published data of 1.33,⁵¹ and $n_f = 1.35 \pm 0.02$ for the binary $\text{CH}_3\text{OH-CO}$ mixture. The column densities were calculated utilizing a modified Lambert-Beer relationship^{52–54} with the absorption coefficients of 1.3×10^{-17} cm molecule⁻¹ and 1.1×10^{-17} cm molecule⁻¹ for the 1028 cm^{-1} (ν_8 ; CH_3OH) and 2090 cm^{-1} (ν_1 ; ^{13}CO) bands, respectively.^{41,55,56} Accordingly, the mixed methanol-carbon monoxide ice was found to be in the ratio of $(4.0 \pm 0.2) : (5.0 \pm 0.2)$. In addition, isotopically-labeled CD_3OD , $^{13}\text{CH}_3\text{OH}$, and $\text{CH}_3^{18}\text{OH}$ ices for pure methanol irradiation experiments and $\text{CD}_3\text{OD-CO}$, $^{13}\text{CH}_3\text{OH-CO}$, $\text{CH}_3^{18}\text{OH-CO}$, $\text{CD}_3\text{OD-}^{13}\text{CO}$, $\text{CH}_3^{18}\text{OH-C}^{18}\text{O}$, and $\text{CH}_3\text{OH-C}^{18}\text{O}$ mixed ices for methanol-carbon monoxide irradiation experiments were also used to confirm infrared assignments *via* isotope shifts, and in the reflectron time-of-flight data *via* shifts their in mass-to-charge ratios.

Each of the amorphous ices was irradiated with 5 keV electrons isothermally at 5.5 ± 0.1 K for one hour at 30 nA over a square area of $1.0 \pm 0.1\text{ cm}^2$ and at an angle of 70° relative to the surface normal. The emission current was measured prior to irradiation on line and *in situ* utilizing a Faraday cup (Kimball Physics, FC-71) mounted inside a differentially pumped chamber on an ultra-high vacuum compatible translation stage. The total dose deposited into the ice sample was determined from Monte Carlo simulations (CASINO)⁵⁷ taking into consideration the scattering coefficient and the energy deposited from the back scattered electrons. The total energy deposited into the amorphous ice was 6.5 ± 0.8 eV per CH_3OH molecule, and 5.2 ± 0.8 eV per molecule on average for the irradiation experiments of the binary $\text{CH}_3\text{OH-CO}$ (4 : 5) ice mixture. It should be noted here that in determining the applied dose of the isotopic analogs, that both the index of refraction and density were assumed to be that of their respective normal counterparts, as most of these data are not empirically available. Furthermore, the density of the $\text{CH}_3\text{OH-CO}$ ice mixture was calculated to be 1.026 g cm^{-3} based on the column density weighted fraction of their respective pure densities (1.020 g cm^{-3} CH_3OH , 1.029 g cm^{-3} CO^{41}) in the limit of volume additivity.⁵⁸

For the on line and *in situ* identification of new molecular band carriers of the ices during irradiation, a Fourier transform infrared spectrometer (Nicolet 6700) monitored the samples throughout the duration of the experiment, with an IR spectrum collected every two minutes in the range of 6000–400 cm^{-1} at a resolution of 4 cm^{-1} . Each FTIR spectrum was recorded in the absorption–reflection–absorption mode (reflection angle = 45°) for two minutes, resulting in a set of 30 infrared spectra during the radiation exposure for each system. We recognize that integrated band areas can be altered by optical interference effects inherent in absorption–reflection–absorption FTIR spectroscopy, as demonstrated by Teolis *et al.*;⁵⁹ however, this issue is circumvented by integration of weak bands, whose absorbance remains linear with respect to the amount of ice deposited.⁶⁰ After the irradiation, the sample was kept at 5.5 K for one hour, then temperature programmed desorption (TPD) studies were conducted by heating the irradiated ices at a rate of 0.5 K min^{-1} to 300 K. Throughout the thermal sublimation process, the ice samples were monitored *via* infrared spectroscopy and single photon ionization reflectron time-of-flight mass spectroscopy⁶¹ separately, *i.e.* each experiment was conducted twice. For the gas phase detection, the products were ionized upon sublimation *via* single photon ionization exploiting pulsed (30 Hz) coherent vacuum ultraviolet (VUV) light at 118.2 nm (10.49 eV), generated *via* non-linear four wave mixing. The ions were then extracted into a reflectron time-of-flight mass spectrometer, whereupon the ions were mass resolved according to their arrival times. Please see the ESI† for more detailed description regarding CASINO calculations, coherent VUV light generation, and reflectron time-of-flight mass spectroscopy.

3. Results

3.1 Infrared spectroscopy

3.1.1 Qualitative analysis. The infrared spectra of pure methanol ice and mixed ices of methanol (CH_3OH)–carbon monoxide (CO) recorded before and after irradiation along with the assignments are shown in Fig. 2A and 2B. During the irradiation, multiple new absorption features emerged (summarized in the ESI, Tables S2 and S3†) alongside the absorptions of the pristine ices. In the irradiated methanol (Fig. 2A, ESI Table S2†) and methanol–carbon monoxide ices (Fig. 2B, ESI Table S3†), the hydroxymethyl radical (CH_2OH) was detected *via* the ν_4 absorption band at 1192 cm^{-1} and 1193 cm^{-1} , respectively, in good agreement with previously reported values of 1197 cm^{-1} in UV photolyzed methanol ices by Gerakines *et al.*,³⁹ 1197 cm^{-1} and 1192 cm^{-1} in methanol⁴⁰ and methanol–carbon monoxide ices⁴¹ exposed to electron irradiation, and 1193 cm^{-1} in methanol ices irradiated with soft X-rays by Chen *et al.*⁴⁴ Formaldehyde (H_2CO) was observed *via* the ν_2 , ν_3 , and ν_4 absorption bands at 1246 cm^{-1} , 1499 cm^{-1} and 1726 cm^{-1} in methanol ice, and at 1249 cm^{-1} , 1497 cm^{-1} and 1726 cm^{-1} in methanol–carbon monoxide ice; again, these absorptions agree with previous studies.^{37,39–41} Methyl formate (HCOOCH_3) was identified *via* its ν_{14} fundamental at 1714 cm^{-1} , which is in good agreement with the literature value of 1718 cm^{-1} in electron irradiation experiments with methanol⁴⁰ and methanol–carbon monoxide ices⁴¹ and UV photolysis of methanol ices by Gerakines *et al.*,³⁹ and 1720 cm^{-1} by Modica *et al.* with pure methyl formate spectra at 16 K.^{42,43} The formation of a formyl radical (HCO) was identified *via* the ν_3 fundamental at 1842 cm^{-1} in both the irradiated

ices, as previously assigned at 1848 cm^{-1} by Hudson *et al.*,³⁷ and at 1842 cm^{-1} by Bennett *et al.*^{40,41} and Chen *et al.*^{39,44} Methane (CH_4) was detected *via* the ν_4 fundamental at 1304 cm^{-1} and 1303 cm^{-1} in the methanol and methanol-carbon monoxide ices, respectively. Formation of carbon monoxide (CO) was confirmed *via* the ν_1 fundamental at 2135 cm^{-1} in methanol ice. In addition, carbon dioxide was detected *via* the ν_3 mode at 2339 cm^{-1} in irradiated methanol ice and 2342 cm^{-1} in the irradiated methanol-carbon monoxide ice. Ethylene glycol was identified in both irradiated ices *via* the ν_9 fundamental at 1094 cm^{-1} , based on the assignment of this molecule in previous studies of irradiated methanol ices^{37,40} at 1090 cm^{-1} and 1088 cm^{-1} . It should be mentioned that all other relatively strong infrared absorption bands of ethylene glycol coincidentally overlap with the methanol absorptions^{40,41} and consequently are masked. Glycolaldehyde (HOCH_2CHO) was identified by the ν_{14} (CO of HCO stretching) fundamental at 1743 cm^{-1} in both methanol and methanol-carbon monoxide ices. The assignment of the observed bands to glycolaldehyde are based on previous studies of irradiated methanol⁴⁰ ices at 1747 cm^{-1} , irradiated methanol-carbon monoxide ices⁴¹ at 1757 cm^{-1} , and matrix isolation studies of glycolaldehyde at 13 K at 1747 cm^{-1} .^{62,63} A second band at 1062 cm^{-1} in the methanol-carbon monoxide ice can be attributed to the ν_7 fundamental of glycolaldehyde, in agreement with previous studies.^{41–43,62,63} The assignment of these absorptions was also confirmed *via* their isotopic shifts in irradiated ices consisting of CD_3OD , $^{13}\text{CH}_3\text{OH}$ and $\text{CH}_3^{18}\text{OH}$, as compiled in Table S2 in the ESI,† and irradiated binary mixed ices consisting of $\text{CD}_3\text{OD-CO}$, $^{13}\text{CH}_3\text{OH-CO}$, $\text{CH}_3^{18}\text{OH-CO}$, $\text{CD}_3\text{OD-}^{13}\text{CO}$, $\text{CH}_3^{18}\text{OH-C}^{18}\text{O}$ and $\text{CH}_3\text{OH-C}^{18}\text{O}$ as compiled in Table S3 in the ESI.†

3.1.2 Deconvolution of the carbonyl absorption features. The new absorption features connected to the carbonyl functional group in the $1800\text{--}1600\text{ cm}^{-1}$ region are very broad (Fig. 3a and 3b), implying the presence of multiple carriers. Further evidence is obtained from the additional infrared absorption features of the carbonyl band regions in the irradiated mixed isotopic ices, as shown in Figure 3b. These findings suggest the presence of multiple underlying molecular carriers, and possibly different isotopomers (in the mixed isotopic ices) as well. Therefore, the absorption features in $1800\text{--}1600\text{ cm}^{-1}$ were deconvoluted with the peak positions, and their associated assignments are shown in Fig. 3 and listed in Tables 1–3. The rationale behind the assignments is discussed below.

In the case of irradiated methanol (CH_3OH) ices, the deconvolution (Fig. 3a) identified four distinct bands centered at 1743 cm^{-1} , 1726 cm^{-1} , 1714 cm^{-1} and 1697 cm^{-1} . The band at 1743 cm^{-1} is assigned to the ν_{14} band of glycolaldehyde (HOCH_2CHO), as discussed previously based on earlier experimental work.^{40,41,62,63} The absorptions at 1726 cm^{-1} and 1714 cm^{-1} can be linked to the ν_4 fundamental of formaldehyde (H_2CO) and the ν_{14} of methyl formate (HCOOCH_3), which are in good agreement with the literature data at 1726 cm^{-1} and 1718 cm^{-1} , respectively.^{39–43} Finally, the band observed at 1697 cm^{-1} can be attributed to the Fermi resonance splitting of the ν_{14} fundamental and the $2\nu_6$ overtone band of glycolaldehyde.^{41,44,63} To support these assignments, deconvolution of the bands in $1800\text{--}1600\text{ cm}^{-1}$ region for the isotopically labeled ices of CD_3OD , $^{13}\text{CH}_3\text{OH}$, and $\text{CH}_3^{18}\text{OH}$ were also completed. The ν_{14} band of glycolaldehyde (HOCH_2CHO) at 1743 cm^{-1} is expected to show an isotopic shift of 26 cm^{-1} in CD_3OD ices,⁶⁴ 37 cm^{-1} in $^{13}\text{CH}_3\text{OH}$ ices,⁶⁴ and 30 cm^{-1} in $\text{CH}_3^{18}\text{OH}$ ices.⁶⁵ In the present investigation, the corresponding isotopomers of glycolaldehyde, DOCD_2CDO in CD_3OD

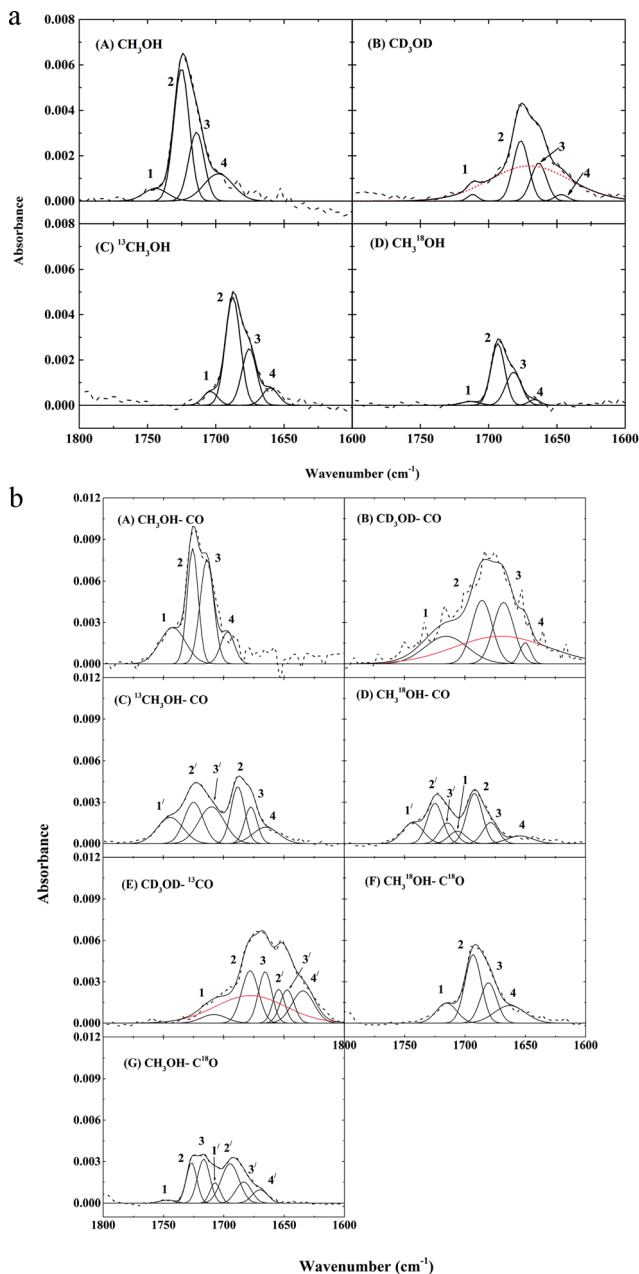


Fig. 3 (a) Deconvoluted infrared absorption features in the region of the carbonyl functional group in (A) CH₃OH, (B) CD₃OD, (C) ¹³CH₃OH, and (D) CH₃¹⁸OH ices. The bands marked as (1) and (4) are assigned as the ν₁₄ and 2ν₆ bands of glycolaldehyde (HOCH₂CHO), respectively. The bands marked as (2) and (3) are assigned to formaldehyde (H₂CO) and methyl formate (HCOOCH₃). The dotted line in (B) corresponds to 2ν₈ of CD₃OD as in the pristine ice. (b) Deconvoluted infrared absorption features in the region of the carbonyl functional group in (A) CH₃OH-CO, (B) CD₃OD-CO, (C) ¹³CH₃OH-CO, (D) CH₃¹⁸OH-CO, (E) CD₃OD-¹³CO, (F) CH₃¹⁸OH-C¹⁸O, and (G) CH₃OH-C¹⁸O ices. The bands marked as (1), (2), (3) and (4) are assigned to ν₁₄ of glycolaldehyde, ν₄ of formaldehyde and ν₁₄ of methyl formate, and 2ν₆ bands of glycolaldehyde and their isotopomers (Table 3), respectively.⁴¹ In

ices, $\text{HO}^{13}\text{CH}_2^{13}\text{CHO}$ in $^{13}\text{CH}_3\text{OH}$ ices, and $\text{H}^{18}\text{OCH}_2\text{CH}^{18}\text{O}$ in $\text{CH}_3^{18}\text{OH}$ ices, are assigned based on peak positions of 1711 cm^{-1} , 1703 cm^{-1} and 1713 cm^{-1} , respectively, with corresponding isotopic shifts of 32 cm^{-1} , 40 cm^{-1} and 30 cm^{-1} (Table 1), in agreement with the expected frequency shifts.^{64,65} The formaldehyde identification was based on the ν_4 band, observed at 1676 , 1687 and 1693 cm^{-1} in the irradiated CD_3OD , $^{13}\text{CH}_3\text{OH}$ and $\text{CH}_3^{18}\text{OH}$ ices, respectively. The corresponding isotopic shifts of 50 , 39 and 33 cm^{-1} agree well with the respective literature values^{66,67} of 45 , 38 and 33 cm^{-1} . Methyl formate was confirmed *via* the ν_{14} band at 1676 cm^{-1} and 1682 cm^{-1} in $^{13}\text{CH}_3\text{OH}$ and $\text{CH}_3^{18}\text{OH}$ ices, with isotopic shifts of 38 cm^{-1} and 32 cm^{-1} respectively, in close agreement with typical shifts of carbonyl stretching frequencies upon ^{13}C and ^{18}O substitution of about 40 cm^{-1} and 30 cm^{-1} , respectively.⁶⁵ In addition, the band assigned to the Fermi resonance (of the ν_{14} fundamental and an overtone from $2\nu_6$) also shows relevant isotopic shifts (Table 1).⁶⁵

The deconvoluted absorption bands of the carbonyl functional group in the $1800\text{--}1600\text{ cm}^{-1}$ region reveal four distinct bands (Figure 3a) in the case of isotopically pure (only one isotope of each atom) binary ices consisting of $\text{CH}_3\text{OH}\text{--CO}$, $\text{CD}_3\text{OD}\text{--CO}$ and $\text{CH}_3^{18}\text{OH}\text{--C}^{18}\text{O}$, similar to that of the irradiated pure methanol ices. Here, the glycolaldehyde isotopomers HOCH_2CHO , DOCD_2CDO and $\text{H}^{18}\text{OCH}_2\text{CH}^{18}\text{O}$ were identified at 1743 cm^{-1} , 1714 cm^{-1} and 1715 cm^{-1} (Table 2), respectively, in excellent agreement with the assigned bands of the corresponding isotopomers observed in irradiated methanol ices (Table 1). However, in the mixed isotopic ices, *i.e.*, $^{13}\text{CH}_3\text{OH}\text{--CO}$, $\text{CH}_3^{18}\text{OH}\text{--CO}$, $\text{CD}_3\text{OD}\text{--}^{13}\text{CO}$ and $\text{CH}_3\text{OH}\text{--C}^{18}\text{O}$, where two different atomic isotopes ($^{12}\text{C}/^{13}\text{C}$ and $^{16}\text{O}/^{18}\text{O}$) are present together, the profile of the carbonyl band was rather unique. Here, evidence of two different isotopomers of glycolaldehyde is observed in the irradiated ices of the mixed isotopes. Fig. 4 presents the isotopomers of glycolaldehyde in these mixed isotopic ices, showing that at least two different carbonyl functional groups could be formed and subsequently detected in the relevant infrared spectral region. For example, $\text{H}^{13}\text{C}^{16}\text{O}$ and $\text{H}^{12}\text{C}^{16}\text{O}$ following irradiation of the $^{13}\text{CH}_3\text{OH}\text{--CO}$ system, $\text{H}^{12}\text{C}^{18}\text{O}$ and $\text{H}^{12}\text{C}^{16}\text{O}$ in the $\text{CH}_3^{18}\text{OH}\text{--CO}$ system, $\text{D}^{12}\text{C}^{16}\text{O}$ and $\text{D}^{13}\text{C}^{16}\text{O}$ in the $\text{CD}_3\text{OD}\text{--}^{13}\text{CO}$ system, and $\text{H}^{12}\text{C}^{16}\text{O}$ and $\text{H}^{12}\text{C}^{18}\text{O}$ in the $\text{CH}_3\text{OH}\text{--C}^{18}\text{O}$ system are expected and can ultimately lead to the synthesis of four different isotopomers of glycolaldehyde. For instance, in the case of irradiated $\text{CH}_3^{18}\text{OH}\text{--CO}$ ice, four different isotopomers of glycolaldehyde, $\text{H}^{18}\text{OCH}_2\text{CH}^{18}\text{O}$, $\text{H}^{18}\text{OCH}_2\text{CHO}$, $\text{HOCH}_2\text{CH}^{18}\text{O}$ and HOCH_2CHO , can be formulated. Here, the carbonyl group (HC^{18}O) in $\text{H}^{18}\text{OCH}_2\text{CH}^{18}\text{O}$ and $\text{HOCH}_2\text{CH}^{18}\text{O}$ can be formed *via* the decomposition of $\text{CH}_3^{18}\text{OH}$. Furthermore, the carbonyl unit (HCO), in $\text{H}^{18}\text{OCH}_2\text{CHO}$ and HOCH_2CHO can be synthesized *via* the hydrogenation of the carbon monoxide (CO). Note that, despite the existence of four different isotopomers, the ν_{14} (CO stretching of the HCO unit) fundamental band will only indicate two glycolaldehyde isotopomers, as in the $\text{CH}_3^{18}\text{OH}\text{--C}^{18}\text{O}$ (1715 cm^{-1}) and $\text{CH}_3\text{OH}\text{--CO}$ (1743 cm^{-1}) ices. Unfortunately, the isotopic combination is attributed to the alcohol vibrational mode, and is consequently masked by the

(C), (D), (E) and (G), the bands marked as (1'), (2'), (3') and (4') are assigned to ν_{14} of glycolaldehyde, ν_4 of formaldehyde, ν_{14} of methyl formate, and $2\nu_6$ bands of glycolaldehyde and their isotopomers, respectively. The dotted lines in (B) and (E) correspond to $2\nu_8$ of CD_3OD as in the pristine ice.

Table 1 Deconvoluted peak positions of the carbonyl absorption bands observed in the processed CH₃OH, CD₃OD, ¹³CH₃OH, and CH₃¹⁸OH ices

| Band | CH ₃ OH (cm ⁻¹) | CD ₃ OD (cm ⁻¹) | Δν (cm ⁻¹) | ¹³ CH ₃ OH (cm ⁻¹) | Δν (cm ⁻¹) | CH ₃ ¹⁸ OH (cm ⁻¹) | Δν (cm ⁻¹) | Assignment |
|------|-------------------------------------------|-------------------------------------------|---------------------------|---------------------------------------------------------|---------------------------|---------------------------------------------------------|---------------------------|-----------------------------------------|
| 1 | 1743 | 1711 | -32 | 1703 | -40 | 1713 | -30 | ν ₁₄ (HOCH ₂ CHO) |
| 2 | 1726 | 1676 | -50 | 1687 | -39 | 1693 | -33 | ν ₄ (H ₂ CO) |
| 3 | 1714 | 1664 | -50 | 1676 | -38 | 1682 | -32 | ν ₁₄ (HCOOCH ₃) |
| 4 | 1697 | 1647 | -50 | 1659 | -38 | 1666 | -31 | 2ν ₆ (HOCH ₂ CHO) |

Table 2 Deconvoluted peak positions of the carbonyl absorption bands observed in the processed isotopically pure ices CH₃OH-CO, CD₃OD-CO, and CH₃¹⁸OH-C¹⁸O

| Band | CH ₃ OH-CO (cm ⁻¹) | CD ₃ OD-CO (cm ⁻¹) | Δν (cm ⁻¹) | CH ₃ ¹⁸ OH-C ¹⁸ O (cm ⁻¹) | Δν (cm ⁻¹) | Assignment |
|------|----------------------------------------------|----------------------------------------------|---------------------------|---------------------------------------------------------------------------|---------------------------|-----------------------------------------|
| 1 | 1743 | 1714 | -29 | 1715 | -28 | ν ₁₄ (HOCH ₂ CHO) |
| 2 | 1726 | 1686 | -40 | 1693 | -33 | ν ₄ (H ₂ CO) |
| 3 | 1714 | 1668 | -46 | 1680 | -34 | ν ₁₄ (HCOOCH ₃) |
| 4 | 1697 | 1651 | -46 | 1662 | -35 | 2ν ₆ (HOCH ₂ CHO) |

broad parent methanol feature. Indeed, deconvolution of the carbonyl absorption in the 1800–1600 cm⁻¹ region of irradiated CH₃¹⁸OH-CO ices (Fig. 3b) resulted in identified bands at 1708 cm⁻¹ (band 1) and 1743 cm⁻¹ (band 1'), which are in close agreement with the expected frequencies based on the isotopically labeled pure ices as mentioned above. Similar to the irradiated CH₃¹⁸OH-CO ices, deconvolution of the mixed isotopic ices of ¹³CH₃OH-CO, CD₃OD-¹³CO and CH₃OH-C¹⁸O reveal two distinct carbonyl bands as shown in Fig. 3b, with the assignments also listed in Table 3. Here, in the isotopically labeled ¹³CH₃OH-CO irradiated ices, the ν₁₄ fundamental of glycolaldehyde isotopomers with H¹³CO and HCO functional groups are expected at 1703 cm⁻¹ and 1743 cm⁻¹, based on the observed band positions in the irradiated ¹³CH₃OH ices and CH₃OH-CO ices. As expected, deconvolution elucidates a band at 1743 cm⁻¹ (band 1') corresponding to the carbon monoxide hydrogenation products. Unfortunately however, the expected band at 1703 cm⁻¹ could not be identified due to a strong transition of the ν₁₄ fundamental of methyl formate (HCOO¹³CH₃) at 1710 cm⁻¹ (band 3'). In CD₃OD-¹³CO ices, the deconvolution of the relevant 1800–1600 cm⁻¹ region required the inclusion of the 2ν₈ overtone band of CD₃OD (1666 cm⁻¹, ESI Table S3†). Consequently, any prediction may result in an ambiguous interpretation. However, the fully deuterated isotopomers of glycolaldehyde with the DCO carbonyl functional group (Fig. 4) can be attributed to the band observed at 1709 cm⁻¹ (band 1), in agreement with irradiated CD₃OD-CO ices (1714 cm⁻¹). Finally, in CH₃OH-C¹⁸O ices, the ν₁₄ fundamental of the glycolaldehyde isotopomers with HCO and HC¹⁸O carbonyl functional groups are expected at 1715 cm⁻¹ and 1743 cm⁻¹, based on the observed band positions in the irradiated CH₃¹⁸OH-C¹⁸O and CH₃OH-CO ices. Certainly, deconvolution reveals two bands centered at 1707 cm⁻¹ (band 1') and 1747 cm⁻¹ (band 1), which are in close agreement with our expectations based on the irradiated isotopically pure ices as mentioned above.

Table 3 Deconvoluted peak positions of the carbonyl absorption bands observed in the processed isotopically mixed ices: $^{13}\text{CH}_3\text{OH}-\text{CO}$, $\text{CH}_3^{18}\text{OH}-\text{CO}$, $\text{CD}_3\text{OD}-^{13}\text{CO}$, and $\text{CH}_3^{18}\text{OH}-\text{CO}$

| Bands | $^{13}\text{CH}_3\text{OH}-\text{CO}$ (cm^{-1}) | $\Delta\nu$ (cm^{-1}) | $\text{CH}_3^{18}\text{OH}-\text{CO}$ (cm^{-1}) | $\Delta\nu$ (cm^{-1}) | $\text{CD}_3\text{OD}-^{13}\text{CO}$ (cm^{-1}) | $\Delta\nu$ (cm^{-1}) | $\text{CH}_3\text{OH}-\text{C}^{18}\text{O}$ (cm^{-1}) | $\Delta\nu$ (cm^{-1}) | Assignment |
|-------|---------------------------------------------------------------|-------------------------------------|---------------------------------------------------------------|-------------------------------------|---------------------------------------------------------------|-------------------------------------|----------------------------------------------------------------------|-------------------------------------|--------------------------------------------|
| 1 | — | — | 1708 | -35 | 1709 | -34 | 1747 | 3 | ν_{14} (HOCH_2CHO) |
| 1' | 1743 | 0 | 1743 | 0 | — | — | 1707 | -36 | |
| 2 | 1692 | -34 | 1692 | -34 | 1678 | -48 | 1726 | 0 | ν_4 (H_2CO) |
| 2' | 1724 | -2 | 1724 | -2 | 1655 | -71 | 1695 | -31 | |
| 3 | 1678 | -36 | 1680 | -34 | 1666 | -48 | 1716 | 2 | ν_{14} (HCOOCH_3) |
| 3' | 1710 | -4 | 1714 | 0 | 1647 | -67 | 1684 | -30 | |
| 4 | 1664 | -33 | — | — | — | — | — | — | $2\nu_6$ (HOCH_2CHO) (?) |
| 4' | — | — | 1654 | -43 | 1633 | -64 | 1670 | -27 | |

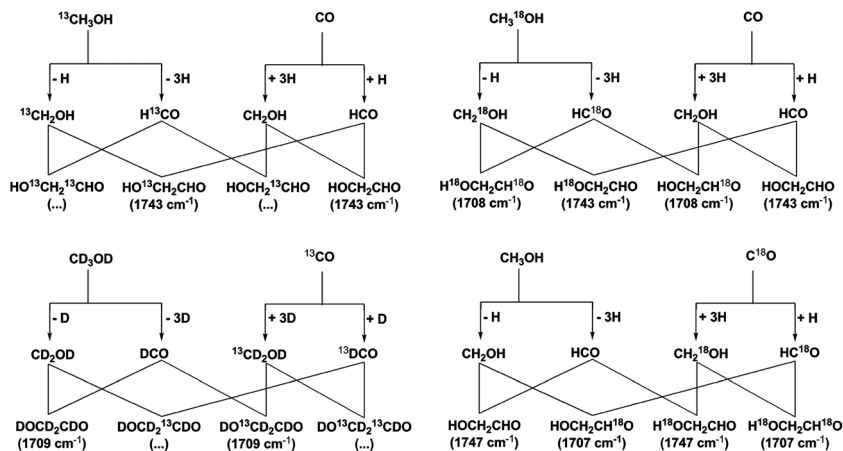


Fig. 4 Schematic representation of the formation of glycolaldehyde isotopomers in mixed isotopic ices of $^{13}\text{CH}_3\text{OH}-\text{CO}$, $\text{CH}_3^{18}\text{OH}-\text{CO}$, $\text{CD}_3\text{OH}-^{13}\text{CO}$ and $\text{CH}_3\text{OH}-\text{C}^{18}\text{O}$. Here, two different carbonyl functional units ($\text{H}^{13}\text{C}^{16}\text{O}$ and $\text{H}^{12}\text{C}^{16}\text{O}$ in $^{13}\text{CH}_3\text{OH}-\text{CO}$; $\text{H}^{12}\text{C}^{18}\text{O}$ and $\text{H}^{12}\text{C}^{16}\text{O}$ in $\text{CH}_3^{18}\text{OH}-\text{CO}$; $\text{D}^{12}\text{C}^{16}\text{O}$ and $\text{D}^{13}\text{C}^{16}\text{O}$ in $\text{CD}_3\text{OH}-^{13}\text{CO}$; $\text{H}^{12}\text{C}^{16}\text{O}$ and $\text{H}^{12}\text{C}^{18}\text{O}$ in $\text{CH}_3\text{OH}-\text{C}^{18}\text{O}$) are expected to be observed in each system. The observed peak positions are shown in parentheses.

Fig. 3b and Tables 1–3 also show the identification of ν_4 of the formaldehyde isotopologues, and ν_{14} of the methyl formate isotopologues. In the case of isotopically pure ices of $\text{CH}_3\text{OH}-\text{CO}$, $\text{CD}_3\text{OD}-\text{CO}$ and $\text{CH}_3^{18}\text{OH}-\text{C}^{18}\text{O}$, formaldehyde was confirmed *via* band positions at 1726 cm^{-1} , 1686 cm^{-1} , 1693 cm^{-1} , respectively, and methyl formate bands were observed at 1714 cm^{-1} , 1668 cm^{-1} and 1680 cm^{-1} . Both frequency shifts are in excellent agreement with the observed band positions in the irradiated methanol (isotopically pure) ices (Table 1). Similar to the detection of two different isotopomers of glycolaldehyde in the mixed isotopic ices of $^{13}\text{CH}_3\text{OH}-\text{CO}$, $\text{CH}_3^{18}\text{OH}-\text{CO}$, $\text{CD}_3\text{OD}-^{13}\text{CO}$ and $\text{CH}_3\text{OH}-\text{C}^{18}\text{O}$, two isotopomers of formaldehyde and methyl formate were also observed in the carbonyl stretching regions in each system as expected. Here, H_2CO and H_2^{13}CO were confirmed *via* bands at 1724 cm^{-1} (band 2') and 1692 cm^{-1} (band 2) following irradiation of $^{13}\text{CH}_3\text{OH}-\text{CO}$ ice, in agreement with the observed band positions of H_2CO (1726 cm^{-1}) and H_2^{13}CO (1687 cm^{-1}) in irradiated CH_3OH and $^{13}\text{CH}_3\text{OH}$ ices. Further, after the irradiation of $\text{CH}_3^{18}\text{OH}-\text{CO}$ and $\text{CH}_3\text{OH}-\text{C}^{18}\text{O}$ ices, $\text{H}_2\text{C}^{18}\text{O}$ was observed at 1692 (band 2) and 1695 cm^{-1} (band 2'), respectively, with H_2CO confirmed at 1724 cm^{-1} (band 2') and 1726 cm^{-1} (band 2), respectively. These peak positions agree with the observed positions of formaldehyde in irradiated pure $\text{CH}_3^{18}\text{OH}$ (1693 cm^{-1}) and CH_3OH (1726 cm^{-1}) ices. In irradiated $\text{CD}_3\text{OD}-^{13}\text{CO}$ ices, D_2CO and D_2^{13}CO were observed at 1678 cm^{-1} (band 2) and 1655 cm^{-1} (band 2'), respectively, matching well with the band at 1676 cm^{-1} in irradiated CD_3OD ice, and the literature value for the isotope shift of D_2^{13}CO (71 cm^{-1}) is close to the observed value of 76 cm^{-1} .⁶⁸ Similarly, two isotopomers of methyl formate were also observed in the isotopically mixed ices of methanol-carbon monoxide. Here, HCO and H^{13}CO of methyl formate in the irradiated $^{13}\text{CH}_3\text{OH}-\text{CO}$ ice were detected at 1710 cm^{-1} (band 3') and 1678 cm^{-1} (band 3), which are close to the observed values of methyl formate in CH_3OH (1714 cm^{-1})

and $^{13}\text{CH}_3\text{OH}$ (1676 cm^{-1}) ices. In irradiated $\text{CH}_3^{18}\text{OH-CO}$ and $\text{CH}_3\text{OH-C}^{18}\text{O}$ ices, HC^{18}O units of methyl formate isotopomers were observed at 1680 cm^{-1} (band 3) and 1684 cm^{-1} (band 3'), respectively and the HCO carbonyl unit was observed at 1714 cm^{-1} (band 3') and 1716 cm^{-1} (band 3), respectively. These peak positions agree with the observed positions of methyl formate in irradiated pure $\text{CH}_3^{18}\text{OH}$ (1682 cm^{-1}) and CH_3OH (1714 cm^{-1}) ices. In irradiated $\text{CD}_3\text{OD-}^{13}\text{CO}$ ices, DCO and D^{13}CO carbonyl units of methyl formate were observed at 1666 cm^{-1} (band 3) (1664 cm^{-1} in irradiated CD_3OD ice) and 1647 cm^{-1} (band 3'), respectively. The isotope shift observed in the case of the D^{13}CO (67 cm^{-1}) carbonyl unit in methyl formate is reasonable based on the observed shift in the case of the formaldehyde isotopomer (the $\Delta\nu$ of D_2^{13}CO is 71 cm^{-1}), as discussed earlier.

3.1.3 Quantitative analysis of glycolaldehyde formation. In the case of methanol ices, considering an infrared absorption coefficient of $1.3 \times 10^{-17}\text{ cm molecule}^{-1}$ for the ν_8 band of methanol,⁴⁰ the initial column density of $1.8 \pm 0.2 \times 10^{17}\text{ molecules cm}^{-2}$ decreased to $1.2 \pm 0.2 \times 10^{17}\text{ molecules cm}^{-2}$ after irradiation, with a decrease of $6.0 \pm 0.6 \times 10^{16}$ molecules of methanol (Table 4). During the irradiation by 5 keV electrons with a beam current of 30 nA, a total of 6.7×10^{14} electrons penetrated the sample. From here, we can estimate that 90 ± 9 molecules of methanol were destroyed by each impinging electron, which is equivalent to $1.9 \pm 0.2 \times 10^{-2}\text{ molecules eV}^{-1}$. During the same period of time, $3.1 \pm 0.3 \times 10^{14}$ molecules of glycolaldehyde were produced, with a production rate of $1.0 \pm 0.1 \times 10^{-4}\text{ molecules eV}^{-1}$. The glycolaldehyde abundance is thus calculated to be $0.17 \pm 0.02\%$ with respect to the initial methanol column density. Furthermore, in the case of methanol-carbon monoxide ices, $4.1 \pm 0.4 \times 10^{16}$ molecules of methanol out of $1.1 \pm 0.1 \times 10^{17}\text{ molecules cm}^{-2}$, and $5.4 \pm 0.5 \times 10^{16}$ molecules of carbon monoxide out of $1.8 \pm 0.2 \times 10^{17}\text{ molecules cm}^{-2}$ were destroyed during the irradiation. This leads to the rates of destruction of methanol and carbon monoxide of $1.3 \pm 0.2 \times 10^{-2}$ and $1.8 \pm 0.2 \times 10^{-2}\text{ molecules eV}^{-1}$, respectively. Additionally, $1.6 \pm 0.1 \times 10^{15}$ molecules of glycolaldehyde were produced immediately following irradiation, with an estimated yield of $5.2 \pm 0.5 \times 10^{-4}\text{ molecules eV}^{-1}$. The glycolaldehyde abundance is thus calculated to be $1.4 \pm 0.1\%$ and $0.89 \pm 0.09\%$ with respect to the initial column densities of the methanol and carbon monoxide, respectively. Note that this production rate (molecules eV^{-1}) is almost five times greater than the rate of glycolaldehyde formation in pure methanol ices, suggesting the presence of a more favorable reaction pathway, most probably the hydrogenation of carbon monoxide to the formyl radical, as observed in previous studies.⁴¹

3.2 ReTOF mass spectroscopy

In addition to the detection of glycolaldehyde using FTIR spectroscopy, we employed complementary, highly sensitive single photoionization ReTOF mass spectrometry coupled with temperature programmed desorption (TPD) studies to identify glycolaldehyde in the irradiated methanol ices and mixed methanol-carbon monoxide ices based on the mass-to-charge ratios, the sublimation temperatures and the corresponding shifts in the mass-to-charge ratios upon isotope substitution. Fig. 5A and 5B show the complete ReTOF mass spectra as a function of temperature during the warm-up phase after the irradiation of the methanol and methanol-carbon monoxide ices, respectively. The spectra display

the intensity as total counts of the ionized products subliming into the gas phase at well-defined temperatures.

In the case of the irradiated methanol ices, the molecular formulae of the products can be assigned by tracing the sublimation of the irradiated isotopically labeled ices (D4-methanol (CD_3OD), ^{13}C -methanol ($^{13}\text{CH}_3\text{OH}$) and ^{18}O -methanol ($\text{CH}_3^{18}\text{OH}$)) *via* a shift by 1 amu for each hydrogen (replacing H by D) and carbon (replacing ^{12}C by ^{13}C) atom, and 2 amu for each oxygen (replacing ^{16}O by ^{18}O) atom. Further, the isotopically labeled counterparts can be easily identified in all four ices by plotting the sublimation temperatures *versus* the ion counts and verifying that these species have identical sublimation profiles.^{64,65} In the case of binary ices of methanol–carbon monoxide, in addition to the natural isotopic ices of $\text{CH}_3\text{OH}-\text{CO}$, selected isotopically labeled ices $\text{CD}_3\text{OD}-\text{CO}$, $^{13}\text{CH}_3\text{OH}-\text{CO}$, $\text{CH}_3^{18}\text{OH}-\text{CO}$, $\text{CD}_3\text{OD}-^{13}\text{CO}$, $\text{CH}_3^{18}\text{OH}-\text{C}^{18}\text{O}$ and $\text{CH}_3\text{OH}-\text{C}^{18}\text{O}$ were also exposed to ionizing radiation, and the radiation induced products were analyzed following TPD utilizing ReTOFMS. Here, the molecular formulae of the products were assigned based on the same methodology as discussed above. Further, the present set of isotopic ices helped us to assign whether the C/H/O bearing molecules followed the incorporation of the carbon monoxide unit. As an example, from the results from FTIR spectroscopy (Section 3.1), the carbonyl unit (HCO) of the glycolaldehyde (HOCH_2CHO) product can be formed from both methanol and carbon monoxide. Here, selected mixed isotopically labeled binary ices of $^{13}\text{CH}_3\text{OH}-\text{CO}$, $\text{CH}_3^{18}\text{OH}-\text{CO}$, $\text{CD}_3\text{OD}-^{13}\text{CO}$ and $\text{CH}_3\text{OH}-\text{C}^{18}\text{O}$ were studied to assign the molecular formula along with their formation routes.

3.2.1 Glycolaldehyde (HOCH_2CHO). Specific attention is paid to the detection of glycolaldehyde (HOCH_2CHO) in the interstellar analogous ices of methanol and binary ices of methanol–carbon monoxide. In these irradiated CH_3OH ices and $\text{CH}_3\text{OH}-\text{CO}$ ices, the molecular ion peak of glycolaldehyde ($\text{C}_2\text{H}_4\text{O}_2^+$) is expected at $m/z = 60$ amu. It should be mentioned that with the molecular formula $\text{C}_2\text{H}_4\text{O}_2$, four possible isomers exists with following ionization energies (IE): glycolaldehyde (HOCH_2CHO ; IE = 10.20 eV), ethene-1,2-diol ($\text{HOCH}=\text{CHOH}$; IE = 9.62 eV), methyl formate (HCOOCH_3 ; IE = 10.84 eV) and acetic acid (CH_3COOH ; IE = 10.63 eV). Among these isomers, methyl formate (10.84 eV) and acetic acid (10.63 eV) have ionization energies higher than the energy of the photoionization source (10.49 eV) and therefore do not contribute to the ion signal at $m/z = 60$ amu. However, the other two isomers, glycolaldehyde and ethene-1,2-diol, have ionization energies of 10.20 eV and 9.62 eV, respectively, and therefore can be ionized.

3.2.2 Glycolaldehyde in irradiated methanol ices. First, we would like to discuss the identification of glycolaldehyde in methanol ices. It should be mentioned here that, in ices of methanol isotopologues, molecular ion signals of $\text{C}_2\text{H}_4\text{O}_2$ and its isotopomers are expected at $m/z = 60$ amu ($\text{C}_2\text{H}_4\text{O}_2^+$; CH_3OH ice), $m/z = 64$ amu ($\text{C}_2\text{D}_4\text{O}_2^+$; CD_3OD ice), $m/z = 62$ amu ($^{13}\text{C}_2\text{H}_4\text{O}_2^+$; $^{13}\text{CH}_3\text{OH}$ ice), and at $m/z = 64$ amu ($\text{C}_2\text{H}_4^{18}\text{O}_2^+$; $\text{CH}_3^{18}\text{OH}$ ice). Table 5 shows feasible formation routes of $\text{C}_2\text{H}_4\text{O}_2$ isomers, glycolaldehyde and ethene-1,2-diol, through the recombination of radical reactants (HCO, CH_2OH , and CHOH) which can be formed upon radiolysis of methanol. Here, a glycolaldehyde molecule is formulated *via* the radical–radical combination of one HCO with a CH_2OH radical, and ethene-1,2-diol is formally formed *via* dimerization of CHOH or a tautomerization mechanism of glycolaldehyde.

Table 4 Fractional abundances of glycolaldehyde in methanol and methanol–carbon monoxide ices after the irradiation at 5.5 K, and during the warm up phase at 110 K (maximum value) and 150 K (at the time to sublimation)

| Ice | Irradiation | | Warm up phase | | | |
|---------------------------|------------------------------|------------------------------|------------------------------|------------------------------|------------------------------|------------------------------|
| | 5.5 K | $f(\text{CH}_3\text{OH})$ | 110 K | 150 K | $f(\text{CH}_3\text{OH})$ | $f(\text{CH}_3\text{OH})$ |
| CH_3OH | $3.1 \pm 0.3 \times 10^{14}$ | $1.7 \pm 0.2 \times 10^{-3}$ | $8.0 \pm 0.8 \times 10^{14}$ | $3.2 \pm 0.3 \times 10^{14}$ | $4.4 \pm 0.4 \times 10^{-3}$ | $1.8 \pm 0.2 \times 10^{-3}$ |
| $\text{CH}_3\text{OH-CO}$ | $1.6 \pm 0.1 \times 10^{15}$ | $1.4 \pm 0.1 \times 10^{-2}$ | $2.1 \pm 0.2 \times 10^{15}$ | $6.3 \pm 0.6 \times 10^{14}$ | $1.9 \pm 0.2 \times 10^{-2}$ | $5.7 \pm 0.6 \times 10^{-3}$ |

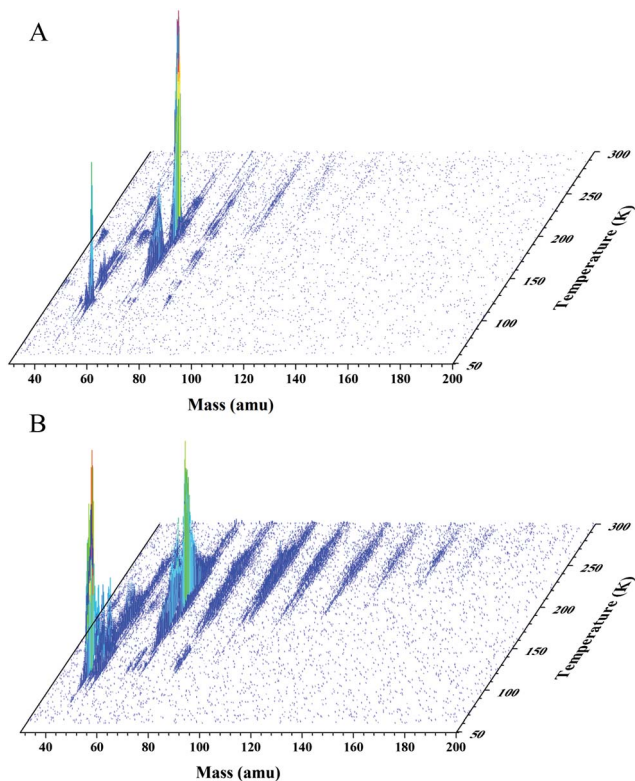


Fig. 5 (A) ReTOF mass spectra as a function of the temperature of the newly formed products subliming into the gas phase from the irradiated methanol (CH_3OH) ices. (B) ReTOF mass spectra as a function of the temperature of the newly formed products subliming into the gas phase from the irradiated methanol–carbon monoxide ($\text{CH}_3\text{OH}-\text{CO}$) ices.

Fig. 6 depicts the sublimation profile of integrated ion counts at $m/z = 60$ amu ($\text{C}_2\text{H}_4\text{O}_2^+$). In principle, the ion signal at $m/z = 60$ amu can also originate from the ionization of $\text{C}_3\text{H}_8\text{O}$ ($m/z = 60$ amu) isomers such as 1-propanol (10.22 eV), 2-propanol (10.17 eV), and methoxyethane (9.72 eV); these molecules have ionization energies lower than the 10.49 eV ionization photon. The distinct peak at 120 K is assigned to $\text{C}_3\text{H}_8\text{O}$ isomers, as observed in previously irradiated CH_4-CO ices.⁶⁵ Furthermore, the pronounced peak at 200 K displays a similar onset to the sublimation profile of $m/z = 62$ amu ($\text{C}_2\text{H}_6\text{O}_2^+$), as shown in Fig. 6. The similarity in the onsets of the sublimation profiles of $m/z = 60$ amu ($\text{C}_2\text{H}_4\text{O}_2^+$) and $m/z = 62$ amu ($\text{C}_2\text{H}_6\text{O}_2^+$) implies that the ion signal at $m/z = 60$ amu ($\text{C}_2\text{H}_4\text{O}_2^+$) could be due to the photofragmentation of the parent $\text{C}_2\text{H}_6\text{O}_2$ molecules. In an effort to explore this possibility, the TPD ReTOF mass spectra of pure ethylene glycol ($\text{HOCH}_2\text{-CH}_2\text{OH}$; IE = 10.16 eV) and a 10% mixture of ethylene glycol in methanol and methanol–carbon monoxide ices were recorded as a function of temperature under identical experimental parameters. Here, ethylene glycol did not exhibit any fragmentation to $m/z = 60$ amu, indicating that co-sublimation of $\text{C}_2\text{H}_4\text{O}_2$ ($m/z = 60$ amu) along with ethylene glycol ($\text{C}_2\text{H}_6\text{O}_2$; $m/z = 62$ amu) is responsible for the signal detected at 200 K.

To verify the identification of $C_2H_4O_2$ isomers, we probed the sublimation of the isotopically substituted counterparts in the irradiated CD_3OD , $^{13}CH_3OH$, and $CH_3^{18}OH$ ices, and explored the expected isotope shifts of glycolaldehyde (Fig. 7). Here, we observed a signal at $m/z = 64$ amu ($C_2D_4O_2^+$) in CD_3OD ice, at $m/z = 62$ amu ($^{13}C_2H_4O_2^+$) in $^{13}CH_3OH$ ice, and at $m/z = 64$ amu ($C_2H_4^{18}O_2^+$) in $CH_3^{18}OH$ ices, and their temperature-dependent sublimation profiles are shown in Fig. 7. Here, the ReTOF sublimation profiles at $m/z = 60$ amu ($C_2H_4O_2^+$) in the CH_3OH system and at $m/z = 64$ amu ($C_2D_4O_2^+$) in the CD_3OD system show five distinct peaks (i–v), whereas the TPD ReTOF sublimation profiles at $m/z = 62$ amu ($^{13}C_2H_4O_2^+$) in the $^{13}CH_3OH$ system and at $m/z = 64$ amu ($C_2H_4^{18}O_2^+$) in the $CH_3^{18}OH$ system show four peaks (ii–v); the assignments of these peaks are listed in Table 6. As discussed earlier, the distinct peak (i) at 120 K in CH_3OH and CD_3OD ices can be assigned to the C_3H_8O ($m/z = 60$ amu) and C_3D_6O ($m/z = 64$ amu) isomers, respectively, as observed in a previous report of irradiated CH_4 –CO ices.⁶⁵ The remaining peaks, labeled as (ii), (iii), (iv), and (v) in Fig. 7, are observed in all the isotopologous ices; the similar sublimation profiles and positions of the peaks in these systems support the formation of $C_2H_4O_2$ isomers. Here, peak (ii), which begins sublimation at 150 ± 2 K with a maximum at 166 ± 2 K, is assigned to glycolaldehyde ($HOCH_2CHO$). To support this assignment, it is important to recall that the formation of glycolaldehyde was also confirmed *via* the detection of a peak at 1743 cm^{-1} (ν_{14}) together with its isotopically labeled counterparts. Furthermore, the ν_{14} integrated band area displays a strong decline at 150 K, which correlates well with the increase in the ReTOF ion signal of the $C_2H_4O_2$ isotopologues at 150 ± 2 K (ESI, Fig. S11†). As we have discussed earlier, the glycolaldehyde absorption band becomes untraceable beyond 175 K, and any sublimation of $m/z = 60$ amu above 175 K cannot be explained by the sublimation of glycolaldehyde, but likely originates from the sublimation of the second isomer

Table 5 Mass-to-charge ratios of $C_2H_4O_2$ isomers along with the radical–radical combination routes in irradiated methanol ices

| Ices | Reactants | Glycolaldehyde | Ethene-1,2-diol |
|---------------|-------------------------------------------|--------------------------------------------------------------|-----------------|
| CH_3OH | HCO (29 amu) | HOCH ₂ CHO (60 amu) | |
| | CH ₂ OH (31 amu) | | |
| | CHOH (30 amu) | x 2 | |
| CD_3OD | DCO (30 amu) | DOCD ₂ CDO (64 amu) | |
| | CD ₂ OD (34 amu) | | |
| | CDOD (32 amu) | x 2 | |
| $^{13}CH_3OH$ | H ¹³ CO (30 amu) | HO ¹³ CH ₂ ¹³ CHO (62 amu) | |
| | ¹³ CH ₂ OH (32 amu) | | |
| | ¹³ CHOH (31 amu) | x 2 | |
| $CH_3^{18}OH$ | HC ¹⁸ O (31 amu) | H ¹⁸ OCH ₂ CH ¹⁸ O (64 amu) | |
| | CH ₂ ¹⁸ OH (33 amu) | | |
| | CH ¹⁸ OH (32 amu) | x 2 | |

ethene-1,2-diol. Correspondingly, we assign peaks (iii) and (iv) at 200 K and 210 K to the sublimation of ethene-1,2-diol (HOCH=CHOH). Recall that the peak at 200 K is due to the co-sublimation of $C_2H_4O_2$ along with ethylene glycol as discussed previously. Note that ethene-1,2-diol, having two OH functional groups, can interact more strongly with ethylene glycol *via* hydrogen bonding, and co-sublimation is therefore reasonable. Furthermore, sublimation of ethene-1,2-diol peaking at 210 K (iv) is also reasonable, as ethene-1,2-diol has a higher polarity compared to glycolaldehyde (HOCH₂CHO). In addition to this, evidence of infrared absorption in the OH stretching region (see Fig. 8) after the complete sublimation of ethylene glycol at around 210 K also suggests the presence of ethene-1,2-diol in the ices, which peaks at 210 K. Finally, the distinct peak at around 234 K (v) can be assigned to fragmentation from glycerol ($C_3H_8O_3$), based on a recent study on the photoionization of glycerol ($C_3H_8O_3$) which identified a prominent photofragment at $m/z = 60$ amu ($C_2H_4O_2$) with an appearance energy of 9.9 eV.⁶⁹ The identification of glycerol in these experiments will be presented in a follow up article, as we are focusing solely on glycolaldehyde here.

3.2.3 Glycolaldehyde in irradiated methanol-carbon monoxide ices. Here we would like to discuss the detection of glycolaldehyde (HOCH₂CHO) during the TPD studies in irradiated methanol-carbon monoxide isotopologue ices. Radical reactants HCO, CH₂OH, and CHOH can be formed once again *via* radiolysis of CH₃OH, or specifically in this system *via* the stepwise hydrogenation of carbon monoxide molecules as shown in Table 7. Note that, in the case of isotopically pure ices, namely CH₃OH-CO, CD₃OD-CO, and CH₃¹⁸OH-C¹⁸O, where only one isotope of each atom is present, $C_2H_4O_2$ isotopologues can only be observed at $m/z = 60$ amu ($C_2H_4O_2^+$), 64 amu ($C_2D_4O_2^+$), and 64 amu ($C_2H_4^{18}O_2^+$), respectively. However, in the case of isotopically mixed ices such as ¹³CH₃OH-CO, CH₃¹⁸OH-CO, CD₃OD-¹³CO and CH₃OH-C¹⁸O, two different isotopes of either carbon (¹²C

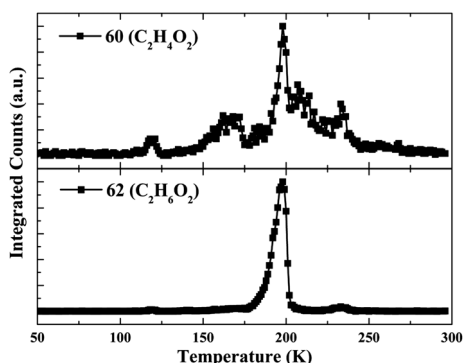


Fig. 6 Top: sublimation profile of integrated counts at $m/z = 60$ amu ($C_2H_4O_2^+$) in the CH₃OH system. Bottom: sublimation profile of $m/z = 62$ amu ($C_2H_6O_2^+$). The pronounced peak at 200 K of $m/z = 60$ amu is a result of the co-sublimation of $C_2H_4O_2$ with $C_2H_6O_2$. The signal at $m/z = 62$ amu ($C_2H_6O_2^+$) is due to ethylene glycol (HOCH₂CH₂OH; 10.16 eV). The distinct peak at 120 K corresponds to C_3H_8O ($m/z = 60$ amu; 1-propanol (10.22 eV), 2-propanol (10.17 eV)), as observed in previous results of irradiated CH₄-CO ices.⁶⁵ Further, the peak at around 234 K is assigned to the fragmentation from higher molecular mass $C_3H_8O_3$ (glycerol), which shows a prominent fragmentation at $m/z = 60$ amu ($C_2H_6O_2^+$, appearance energy 9.9 eV).⁶⁹

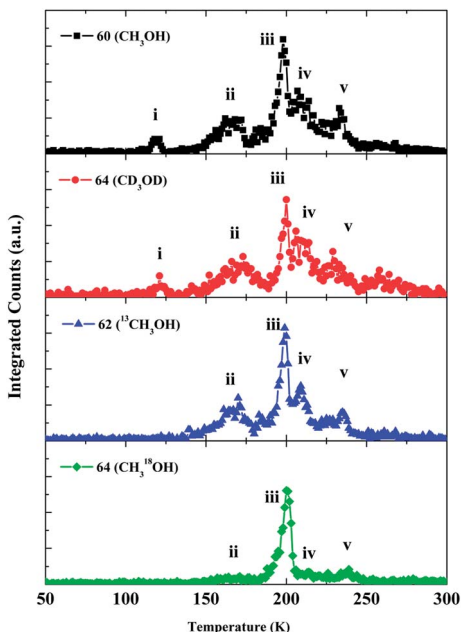


Fig. 7 Sublimation profiles of ion counts at $m/z = 60$ amu ($\text{C}_2\text{H}_4\text{O}_2^+$), 64 amu ($\text{C}_2\text{D}_4\text{O}_2^+$), 62 amu ($^{13}\text{C}_2\text{H}_4\text{O}_2^+$), and 64 amu ($\text{C}_2\text{H}_4^{18}\text{O}_2^+$) in CH_3OH , CD_3OD , $^{13}\text{CH}_3\text{OH}$, and $\text{CH}_3^{18}\text{OH}$ systems, respectively. In the case of CD_3OD ices, the peak at 120 K (i) corresponds to $\text{C}_3\text{D}_6\text{O}$ ($m/z = 64$ amu; acetone (9.7 eV), propanal (10.0 eV)), as observed in a previous report of irradiated $\text{CD}_4\text{-CO}$ ices.⁶⁵ The peak at 200 K is a result of the co-sublimation of $\text{C}_2\text{H}_4\text{O}_2^+$ ($m/z = 60$ amu) with ethylene glycol ($\text{C}_2\text{H}_6\text{O}_2$). Detailed assignments of the peaks (i–v) are listed in Table 6.

and ^{13}C) or oxygen (^{16}O and ^{18}O) are present together; hence two different isotopic sets of radical reactants are possible, as identified *via in situ* FTIR spectroscopy of the processed ices (Section 3.1.2). Here, radical–radical recombination leads to the observation of $\text{C}_2\text{H}_4\text{O}_2$ isotopologues at three different masses are expected to be observed in each system; at $m/z = 60$ amu ($\text{C}_2\text{H}_4\text{O}_2^+$), 61 amu ($\text{C}^{13}\text{CH}_4\text{O}_2^+$) and 62 amu ($^{13}\text{C}_2\text{H}_4\text{O}_2^+$) in the $^{13}\text{CH}_3\text{OH-CO}$ system, at $m/z = 60$ amu ($\text{C}_2\text{H}_4\text{O}_2^+$), 62 amu ($\text{C}_2\text{H}_4\text{O}^{18}\text{O}^+$) and 64 amu ($\text{C}_2\text{H}_4^{18}\text{O}_2^+$) in the $\text{CH}_3^{18}\text{OH-CO}$ system, at $m/z = 66$ amu ($^{13}\text{C}_2\text{D}_4\text{O}_2^+$), 65 amu ($\text{C}^{13}\text{CD}_4\text{O}_2^+$) and 64 amu ($\text{C}_2\text{D}_4\text{O}_2^+$) in the $\text{CD}_3\text{OD-}^{13}\text{CO}$ system, and finally at $m/z = 64$ amu ($\text{C}_2\text{H}_4^{18}\text{O}_2^+$), 62 amu ($\text{C}_2\text{H}_4\text{O}^{18}\text{O}^+$) and 60 amu ($\text{C}_2\text{H}_4\text{O}_2^+$) in the $\text{CH}_3\text{OH-C}^{18}\text{O}$ system. Note that, in all the above cases (Table 7), both glycolaldehyde and ethene-1,2-diol cannot be separated based on isotopic mass shifts; however, we can contemplate their detection in irradiated methanol–carbon monoxide ices.

Fig. 9 depicts the sublimation profile of integrated ion counts at $m/z = 60$ ($\text{C}_2\text{H}_4\text{O}_2^+$) in $\text{CH}_3\text{OH-CO}$ ices. The small peak at 120 K is assigned to $\text{C}_3\text{H}_8\text{O}$ isomers, similar to the result for methanol ices. Here, the sublimation profile of $\text{C}_2\text{H}_6\text{O}_2$ is also presented in Fig. 9, and the peak at 196 ± 2 K can be attributed to the co-sublimation of $\text{C}_2\text{H}_4\text{O}_2$ isomers along with ethylene glycol ($\text{C}_2\text{H}_6\text{O}_2$), as discussed in Section 3.2.2. Note that, in isotopically pure ices of $\text{CH}_3\text{OH-CO}$, $\text{CD}_3\text{OD-CO}$ and $\text{CH}_3^{18}\text{OH-C}^{18}\text{O}$, $\text{C}_2\text{H}_4\text{O}_2$ isotopologues are observed only at $m/z =$

Table 6 Assignment of the ion peaks observed in the sublimation profiles at $m/z = 60, 64, 62,$ and 64 in irradiated $\text{CH}_3\text{OH}, \text{CD}_3\text{OD}, ^{13}\text{CH}_3\text{OH},$ and $\text{CH}_3^{18}\text{OH}$ ices, respectively

| Ice | Ion signal (m/z) | Peak i (120 K) | Peak ii (166 K) | Peak iii (200 K) | Peak iv (210 K) | Peak v (234 K) |
|-----------------------------|----------------------|--------------------------------|---------------------------------------------------|---------------------------------------------------|---------------------------------------------------|--------------------------------------------------------------------------------------------------|
| CH_3OH | 60 | $\text{C}_3\text{H}_6\text{O}$ | HOCH_2CHO | $\text{HOCH}=\text{CHOH}$ | $\text{HOCH}=\text{CHOH}$ | Fragmentation ($\text{C}_2\text{H}_4\text{O}_2$) of $\text{C}_3\text{H}_6\text{O}_3$ |
| CD_3OD | 64 | $\text{C}_3\text{D}_6\text{O}$ | DOCD_2CDO | $\text{DOCD}=\text{CDOD}$ | $\text{DOCD}=\text{CDOD}$ | Fragmentation ($\text{C}_2\text{D}_4\text{O}_2$) of $\text{C}_3\text{D}_6\text{O}_3$ |
| $^{13}\text{CH}_3\text{OH}$ | 62 | — | $\text{HO}^{13}\text{CH}_2^{13}\text{CHO}$ | $\text{HO}^{13}\text{CH}=\text{CHOH}$ | $\text{HO}^{13}\text{CH}=\text{CHOH}$ | Fragmentation ($^{13}\text{C}_2\text{H}_4\text{O}_2$) of $^{13}\text{C}_3\text{H}_6\text{O}_3$ |
| $\text{CH}_3^{18}\text{OH}$ | 64 | — | $\text{H}^{18}\text{OCH}_2\text{CH}^{18}\text{O}$ | $\text{H}^{18}\text{OCH}=\text{CH}^{18}\text{OH}$ | $\text{H}^{18}\text{OCH}=\text{CH}^{18}\text{OH}$ | Fragmentation ($\text{C}_2\text{H}_4^{18}\text{O}_2$) of $\text{C}_3\text{H}_6^{18}\text{O}_3$ |

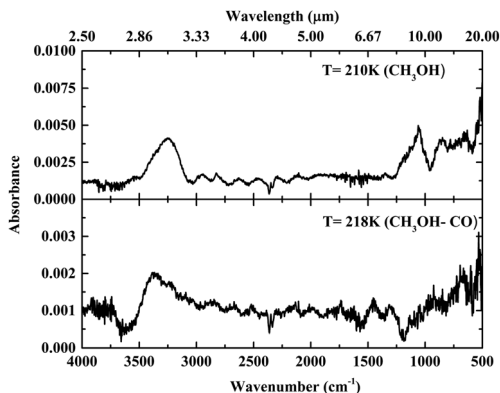


Fig. 8 Infrared absorption spectra of the irradiated methanol (CH_3OH) and methanol-carbon monoxide ($\text{CH}_3\text{OH}-\text{CO}$) ices at 210 K and 218 K. The broad peak from 3500 to 3050 cm^{-1} is assigned to the OH stretching vibrations of alcohols present in the ices. The temperatures of 210 K and 218 K in the CH_3OH and $\text{CH}_3\text{OH}-\text{CO}$ systems correspond to the sublimation of ethene-1,2-diol with ethylene glycol already being sublimed in the gas phase.

60 amu ($\text{C}_2\text{H}_4\text{O}_2^+$), 64 amu ($\text{C}_2\text{D}_4\text{O}_2^+$) and 64 amu ($\text{C}_2\text{H}_4^{18}\text{O}_2^+$), respectively, as derived in Table 7 and shown in Fig. 10. In the case of the $\text{CD}_3\text{OD}-\text{CO}$ system, the peak at 125 K can be assigned to $\text{C}_3\text{D}_6\text{O}$ ($m/z = 64$ amu) isomers. Furthermore, the sublimation profiles of $\text{C}_2\text{H}_4\text{O}_2$ isotopologues depict two distinct peaks at 196 ± 2 K and 218 ± 2 K. The maximum at 196 ± 2 K is assigned to the sublimation of glycolaldehyde. To support these assignments, we recall that the formation of glycolaldehyde was also confirmed *via* the detection of peaks at 1743 cm^{-1} (ν_{14}) and 1062 cm^{-1} (ν_7) in the post-irradiated ices of methanol-carbon monoxide, together with the expected frequency shifts of the isotopically labeled counterparts. The integrated infrared absorption band area of glycolaldehyde at 1743 cm^{-1} (ν_{14}) shows a slow decline in column density at 150 K, followed by a rapid decline at 180 ± 2 K (ESI, Fig. S11[†]). Note that in ESI Fig. S12,[†] the sublimation profiles derived from TPD ReTOF spectroscopy correlate well with the slow (150 K) and then fast (178 ± 2 K) sublimation of glycolaldehyde observed in the FTIR data. However, the peak at 218 ± 2 K cannot be explained by the sublimation of glycolaldehyde, as no trace of glycolaldehyde can be observed in the infrared spectra after 195 K. Here, the peak at 218 ± 2 K is likely to be due to the sublimation of ethene-1,2-diol. As discussed earlier, ethene-1,2-diol is expected to sublimate at a higher temperature due to its higher polarity, and correspondingly stronger intermolecular interactions. Furthermore, the infrared spectrum at 218 K (Fig. 8) shows evidence of absorption in the OH stretching region, which suggests the presence of ethene-1,2-diol, and thus is attributed to the peak at 218 K, as shown in Fig. 9.

4. Discussion

We would like to discuss now the formation mechanisms of glycolaldehyde. The formation routes are based on the empirical evidence presented above, *i.e.* the observation of distinct isotopomers of glycolaldehyde following irradiation within

Table 7 Mass-to-charge ratios of the C₂H₄O₂ isomers, along with the radical–radical combination routes in irradiated methanol–carbon monoxide ices

| Ices | Reactants | Glycolaldehyde | Ethene-1,2-diol |
|----------------------------------|-------------------------------------------|--------------------------------------------------------------|--------------------------------------------------|
| CO + | HCO (29 amu) | HOCH ₂ CHO (60 amu) | |
| | CH ₂ OH (31 amu) | | |
| CH ₃ OH | CHOH (30 amu) | | HOCH=CHOH (60 amu) |
| | | x 2 | |
| CO + | DCO (30 amu) | DOCD ₂ CDO (64 amu) | |
| | CD ₂ OD (34 amu) | | |
| CD ₃ OD | CDOD (32 amu) | | DOCD=CDOD (64 amu) |
| | | x 2 | |
| CO + | HCO (29 amu) | HOCH ₂ CHO (60 amu) | |
| | CH ₂ OH (31 amu) | HO ¹³ CH ₂ CHO (61 amu) | |
| | CHOH (30 amu) | HOCH ₂ ¹³ CHO (61 amu) | |
| ¹³ CH ₃ OH | H ¹³ CO (30 amu) | HO ¹³ CH ₂ ¹³ CHO (62 amu) | HOCH=CHOH (60 amu) |
| | ¹³ CH ₂ OH (32 amu) | | |
| | ¹³ CHOH (31 amu) | | |
| | | x 2 | HOCH= ¹³ CHOH (61 amu) |
| | | x 2 | HO ¹³ CH= ¹³ CHOH (62 amu) |
| CO + | HCO (29 amu) | HOCH ₂ CHO (60 amu) | |
| | CH ₂ OH (31 amu) | H ¹⁸ OCH ₂ CHO (62 amu) | |
| | CHOH (30 amu) | HOCH ₂ CH ¹⁸ O (62 amu) | |
| CH ₃ ¹⁸ OH | HC ¹⁸ O (31 amu) | H ¹⁸ OCH ₂ CH ¹⁸ O (64 amu) | HOCH=CHOH (60 amu) |
| | CH ₂ ¹⁸ OH (33 amu) | | |
| | CH ¹⁸ OH (32 amu) | | |
| | | x 2 | HOCH=CH ¹⁸ OH (62 amu) |
| | | x 2 | H ¹⁸ OCH=CH ¹⁸ OH (64 amu) |
| ¹³ CO + | D ¹³ CO (31 amu) | DO ¹³ CD ₂ ¹³ CDO (66 amu) | |
| | ¹³ CD ₂ OD (35 amu) | DOCD ₂ ¹³ CDO (65 amu) | |
| | ¹³ CDOD (33 amu) | DO ¹³ CD ₂ CDO (65 amu) | |
| CD ₃ OD | DCO (30 amu) | DOCD ₂ CDO (64 amu) | DO ¹³ CD= ¹³ CDOD (66 amu) |
| | CD ₂ OD (34 amu) | | |
| | CDOD (32 amu) | | |
| | | x 2 | DO ¹³ CD=CDOD (65 amu) |
| | | x 2 | DOCD=CDOD (64 amu) |
| C ¹⁸ O + | HC ¹⁸ O (31 amu) | H ¹⁸ OCH ₂ CH ¹⁸ O (64 amu) | |
| | CH ₂ ¹⁸ OH (33 amu) | | |
| CH ₃ ¹⁸ OH | CH ¹⁸ OH (32 amu) | | H ¹⁸ OCH=CH ¹⁸ OH (64 amu) |
| | | x 2 | |
| C ¹⁸ O + | HC ¹⁸ O (31 amu) | H ¹⁸ OCH ₂ CH ¹⁸ O (64 amu) | |
| | CH ₂ ¹⁸ OH (33 amu) | HOCH ₂ CH ¹⁸ O (62 amu) | |
| | CH ¹⁸ OH (32 amu) | H ¹⁸ OCH ₂ CHO (62 amu) | |
| CH ₃ OH | HCO (29 amu) | HOCH ₂ CHO (60 amu) | H ¹⁸ OCH=CH ¹⁸ OH (64 amu) |
| | CH ₂ OH (31 amu) | | |
| | CHOH (30 amu) | | |
| | | x 2 | H ¹⁸ OCH=CHOH (62 amu) |
| | | x 2 | HOCH=CHOH (60 amu) |

isotopically mixed ices, and in conjunction with previously identified routes guided by the kinetic modeling and numerical fitting of the temporal evolution of newly formed products in irradiated ices of methanol⁴⁰ and methanol–carbon

monoxide ices⁴¹ (Fig. 11). In the case of methanol ices, irradiation induced decomposition of methanol follows three major competing reaction pathways: (1) unimolecular decomposition to a hydroxymethyl (CH_2OH) radical and a suprathermal hydrogen atom, (2) unimolecular decomposition to a methoxy (CH_3O) radical and a suprathermal hydrogen atom, and (3) decomposition to formaldehyde (H_2CO) and molecular hydrogen (or two hydrogen atoms).



Among these, reaction (3) is the most dominating pathway, having the rate constant $4.4 \times 10^{-4} \text{ s}^{-1}$, which is about six and four times faster than reaction (1) ($k = 6.95 \times 10^{-5} \text{ s}^{-1}$) and reaction (2) ($k = 1.04 \times 10^{-4} \text{ s}^{-1}$),⁴⁰ respectively. Furthermore, both the hydroxymethyl radical and the methoxy radical were found to undergo subsequent unimolecular decomposition to produce formaldehyde and a hydrogen atom, as in reaction (4) and reaction (5), respectively.



Recall that, during the irradiation of all isotopologue ices, infrared absorptions due to the formaldehyde and hydroxymethyl radicals are indeed observed with corresponding frequency shifts. The kinetic fitting also suggests that formaldehyde is decomposed to form the formyl (HCO) radical and a hydrogen atom (reaction (6)).

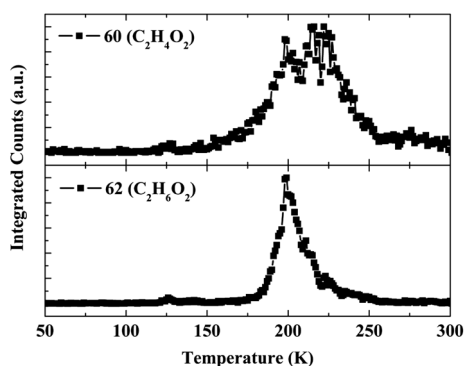


Fig. 9 Top: sublimation profile of ion counts at $m/z = 60$ amu ($\text{C}_2\text{H}_4\text{O}_2^+$) in the $\text{CH}_3\text{OH}-\text{CO}$ system. Bottom: sublimation profile of $m/z = 62$ amu ($\text{C}_2\text{H}_6\text{O}_2^+$), suggesting that the first peak at 198 K in $m/z = 60$ amu is a result of co-sublimation of $\text{C}_2\text{H}_4\text{O}_2$ with ethylene glycol ($\text{C}_2\text{H}_6\text{O}_2$; $\text{HOCH}_2\text{CH}_2\text{OH}$). The peak at 120 K is due to $\text{C}_3\text{H}_8\text{O}$ ($m/z = 60$ amu; 1-propanol (10.22 eV), 2-propanol (10.17 eV)), as observed previously for irradiated CH_4-CO ices.⁶⁵

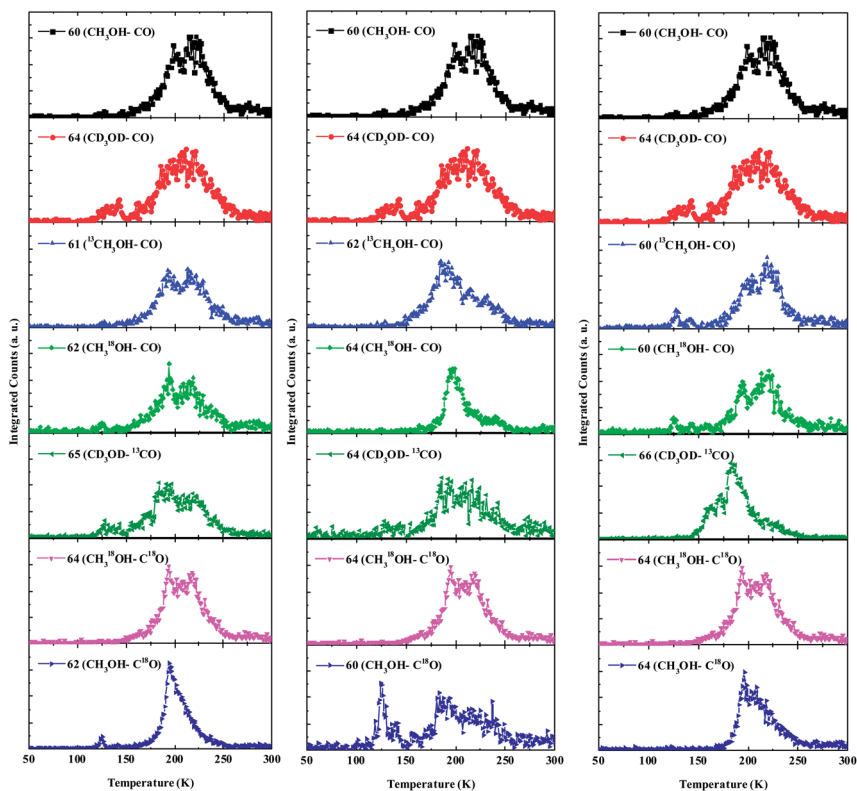


Fig. 10 Sublimation profiles of $C_2H_4O_2$ isotopomers in methanol-carbon monoxide ices. The graphs in the left panel depict the sublimation profile of $C_2H_4O_2$ isotopologues which can be formally formed from one methanol plus one carbon monoxide building block; the graphs in the central panel depict the sublimation profiles of $C_2H_4O_2$ isotopologues which can only be synthesized from two methanol building blocks. The graphs in the right panel show the sublimation profiles of $C_2H_4O_2$ isotopologues which can be formed from two carbon monoxide building blocks. The slight peak at 120 K in the sublimation profiles of $m/z = 60$ amu (CH_3OH-CO) and 62 amu ($CH_3^{18}OH-CO$ and $CH_3OH-C^{18}O$) are due to C_3H_8O and $C_3H_8^{18}O$, respectively. Furthermore, the slight peak at 125 K in the sublimation profiles of $m/z = 64$ amu (CD_3OD-CO), 60 amu ($^{13}CH_3OH-CO$), 60 amu ($CH_3^{18}OH-CO$), 65 amu ($CD_3OD-^{13}CO$) and 60 amu ($CH_3OH-C^{18}O$) are due to C_3D_6O , $C^{13}C_2H_6O$, $C_3H_6^{18}O$, $C_2^{13}CD_6O$, and $C_3H_6^{18}O$, respectively, as observed previously for irradiated CH_4-CO ices.⁶⁵

Finally, the barrierless recombination of the formyl radical with the hydroxymethyl radical can lead to the formation of glycolaldehyde (reaction (7)).



It should be mentioned here that radiolysis of CH_3OH to produce a CH_2OH radical and atomic hydrogen requires $4.03 \text{ eV molecule}^{-1}$, and the minimum energy required to produce one HCO radical is $8.06 \text{ eV molecule}^{-1}$.⁴⁰ As such, the energy required to produce one molecule of glycolaldehyde is $12.09 \text{ eV molecule}^{-1}$. Therefore, non-equilibrium chemistry is crucial to drive the formation of glycolaldehyde in low temperature ices.

In the presence of carbon monoxide, suprathreshold atomic hydrogen produced during the decomposition of methanol can overcome the barrier of addition (4.03 eV molecule⁻¹) to the carbon monoxide molecule, leading to the formation of a formyl radical *via* reaction (8), which may be followed by reaction (7) leading to the formation of glycolaldehyde as well.



Note that in binary ices of methanol and carbon monoxide, the formyl radical can be produced *via* at least two different reaction mechanisms, either *via* radiolysis of methanol (reactions (1)–(6)), or *via* hydrogenation of carbon monoxide (reaction (8)). The reaction mechanisms discussed above suggest that, in the mixed isotopic ices, ¹³CH₃OH–CO, CH₃¹⁸OH–CO, CD₃OD–¹³CO and OH–C¹⁸O, two different glycolaldehyde isotopomers can be formed with the CH₂OH unit from methanol building blocks and the HCO unit either from carbon monoxide building blocks or from methanol building blocks. The deconvolution of the carbonyl absorption in the FTIR spectra of these ices indeed revealed the production of glycolaldehyde isotopologues; thereby supporting the mechanism proposed by Bennett *et al.*^{40,41}

In addition to this, successive hydrogenation of carbon monoxide could lead to the formation of a CH₂OH radical unit which can recombine with the HCO radical unit, formed *via* the above mentioned reaction pathways (6) and (8), to form glycolaldehyde as well (see Fig. 11). In this regard, the hydrogenation of the formyl radical (HCO) formed *via* reaction (8) to form formaldehyde (H₂CO), and a subsequent hydrogenation leading to the formation of the CH₂OH radical *via* reaction pathways (9) and (10) is expected, as shown in Fig. 4 and 11.

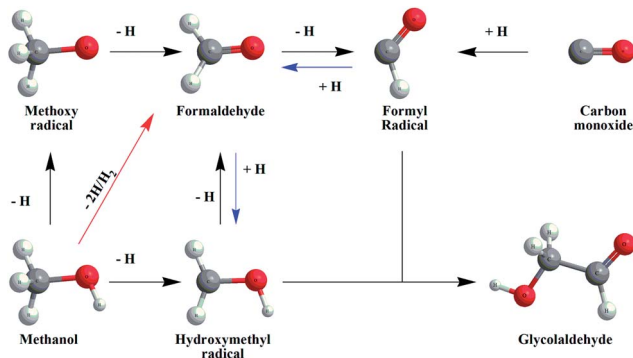
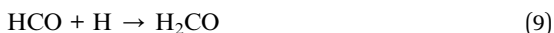


Fig. 11 Reaction scheme for the formation of glycolaldehyde (HOCH₂CHO) in irradiated methanol and in methanol–carbon monoxide mixed ices extracted from the kinetic fittings of the column density of the products. The red arrow indicates the dominant pathway among other pathways for the formation of formaldehyde.^{40,41} The blue arrows indicate additional proposed reaction pathways based on the current experimental results.

Reaction pathway (9) suggests the formation of formaldehyde *via* hydrogenation of carbon monoxide. Recall that, in the mixed isotopic ices of methanol–carbon monoxide, $^{13}\text{CH}_3\text{OH-CO}$, $\text{CH}_3^{18}\text{OH-CO}$, $\text{CD}_3\text{OD-}^{13}\text{CO}$ and $\text{CH}_3\text{OH-C}^{18}\text{O}$, two isotopomers of formaldehyde were observed (Table 3) in each system. As an example, in $\text{CH}_3^{18}\text{OH-CO}$ ices, formaldehyde bands were identified at 1692 cm^{-1} and 1724 cm^{-1} , and these band positions were close to the formaldehyde bands observed in $\text{CH}_3^{18}\text{OH}$ ices ($\text{H}_2\text{C}^{18}\text{O}$; 1693 cm^{-1}) and CH_3OH ices (H_2CO ; 1726 cm^{-1}). Consequently, these observations confirmed the detection of $\text{H}_2\text{C}^{18}\text{O}$ as well as H_2CO at 1692 cm^{-1} and 1724 cm^{-1} , respectively, in $\text{CH}_3^{18}\text{OH-CO}$ ices. The above observation provides clear evidence that reaction pathway (9) occurs. Furthermore, the hydrogenation of formaldehyde to form the CH_2OH radical, followed by recombination with the HCO radical unit (reaction (7)) can result in the formation of glycolaldehyde as well. Note that, in the mixed isotopic ices of methanol–carbon monoxide, two different isotopomers of CH_2OH radicals (*via* reaction pathways (1) and (10)) and two different isotopomers of HCO radicals (reaction pathways (6) and (8)) could lead to the formation of four isotopomers of glycolaldehyde molecules, as shown in Fig. 4. However, within these four isotopomers, only two isotopic carbonyl units (HCO) are present, which results in the detection of two different infrared absorptions of the glycolaldehyde carbonyl stretching vibration in the mixed isotopic ices (Table 3, Fig. 3b). As an example, in the $\text{CH}_3^{18}\text{OH-CO}$ system, CH_2OH , formed *via* the successive hydrogenation of carbon monoxide ((8)–(10)), can recombine with HC^{18}O (*via* reactions (1)–(6)) or HCO (reaction (8)), resulting in $\text{HOCH}_2\text{CH}^{18}\text{O}$ and HOCH_2CHO (see Fig. 4). These two isotopomers have identical carbonyl units of $\text{H}^{18}\text{OCH}_2\text{CH}^{18}\text{O}$ and $\text{H}^{18}\text{OCH}_2\text{CHO}$ (reactions (1)–(8)); consequently, the two carbonyl stretching frequencies detected at 1708 cm^{-1} (HC^{18}O) and 1743 cm^{-1} (HCO) correspond to the respective isotopomers of glycolaldehyde. Based on the *in situ* FTIR and TPD ReTOF mass spectroscopic evidence presented above, the overall reaction pathways ultimately resulting in the formation of glycolaldehyde are presented in Fig. 11.

Also note the increase of glycolaldehyde abundance during the warm up phase of the irradiated ices. Here, the increase of glycolaldehyde was associated with a simultaneous decrease in the amount of formyl radicals. In the case of irradiated methanol ices, the amount of glycolaldehyde increased by almost the exact same amount by which formyl radicals decreased, about 5×10^{14} molecules. Similarly, a corresponding increase in the amount of glycolaldehyde with the decrease in the amount of formyl radicals was observed following the warm up of the irradiated mixed methanol and carbon monoxide ices. Here, the amount of glycolaldehyde increases by a similar order of magnitude (2×10^{14} molecules); however, the amount of formyl radical decreased by almost an order of magnitude more (1.6×10^{15} molecules), accounting for only 12% of the apparent increase in glycolaldehyde, suggesting that an additional chemical route is involved. These observations imply additional thermal chemistry of the trapped radicals diffusing through the methanol matrix following reaction (7), ultimately yielding glycolaldehyde.

5. Conclusions

The present experimental approach specifically focused on the detection of glycolaldehyde in irradiated methanol ices and methanol–carbon monoxide binary

ices along with their isotopically labeled counterparts. Here we utilized two complementary detection techniques, infrared spectroscopy and single photoionization ReTOF mass spectrometry, in order to analyze the endogenous synthesized products formed *via* radiation induced chemical processing. The on line and *in situ* infrared spectroscopy identified the formation of the astrobiologically important molecule glycolaldehyde, based on the agreement of the observed infrared band positions and the associated isotopic shifts with the literature data. In the case of mixed isotopic ices of methanol-carbon monoxide ($^{13}\text{CH}_3\text{OH-CO}$, $\text{CH}_3^{18}\text{OH-CO}$, $\text{CD}_3\text{OD-}^{13}\text{CO}$ and $\text{CH}_3\text{OH-C}^{18}\text{O}$) where two different isotopes of carbon or oxygen are present together, deconvolution of the broad carbonyl absorption features identified at least two isotopomers of glycolaldehyde (Fig. 3B and Table 3). This confirms the presence of at least two reaction pathways in methanol-carbon monoxide ices for the formation of the carbonyl functional group (HCO) of glycolaldehyde, *via* the decomposition of methanol and the hydrogenation of carbon monoxide molecules. Accordingly, during the TPD studies of irradiated methanol and methanol-carbon monoxide ices and their isotopologues, using single photoionization ReTOF mass spectrometry we confirmed the detection of glycolaldehyde based on the identical sublimation profiles of the corresponding shifted masses. Furthermore, the agreement between the sublimation of glycolaldehyde obtained from ReTOF mass spectroscopy and FTIR spectroscopy supports this detection. In the mixed isotopic ices ($^{13}\text{CH}_3\text{OH-CO}$, $\text{CH}_3^{18}\text{OH-CO}$, $\text{CD}_3\text{OD-}^{13}\text{CO}$ and $\text{CH}_3\text{OH-C}^{18}\text{O}$) we were able to detect glycolaldehyde at three different isotopic masses, suggesting that at least three competing reaction mechanisms are involved in the formation of glycolaldehyde in the irradiated ices at 5 K: (i) formation of glycolaldehyde *via* a hydrogenation mechanism of carbon monoxide, (ii) formation of glycolaldehyde *via* the reaction of one methanol unit with carbon monoxide unit, and (iii) *via* the decomposition of a methanol molecule followed by recombination of HCO and CH_2OH radicals.

Upon warming up of the irradiated samples, the column density of the glycolaldehyde shows an increase, implying the presence of additional thermal chemistry, most probably *via* the diffusion and ensuing reaction of trapped radicals. Further, the fractional abundance of the glycolaldehyde in the irradiated methanol ices was estimated (see the ESI for relevant details†) within the range 4.5 ± 0.5 to $1.8 \pm 0.2 \times 10^{-8}$ with respect to molecular hydrogen; in methanol-carbon monoxide ices the fractional abundance of glycolaldehyde is from $1.9 \pm 0.2 \times 10^{-7}$ to $5.7 \pm 0.6 \times 10^{-8}$. These estimated glycolaldehyde abundances are close to the abundances of those calculated based on our observations, with doses relevant to the typical lifetime of interstellar ices prior to the star-formation induced warm up phase. Therefore, our laboratory simulation demonstrates that radiation exposure of bulk ices containing methanol and methanol-carbon monoxide, relevant to the actual physical environment of an ice covered grain mantle, will ultimately lead to the synthesis of glycolaldehyde.

Acknowledgements

The authors would like to thank the W. M. Keck Foundation, the University of Hawaii, and the NASA Exobiology Program MNX13AH62G.

References

- 1 J. M. Hollis, F. J. Lovas and P. R. Jewell, *Astrophys. J.*, 2000, **540**, L107–L110.
- 2 L. E. Snyder, *Proc. Natl. Acad. Sci. U. S. A.*, 2006, **103**, 12243–12248.
- 3 J. M. Hollis, S. N. Vogel, L. E. Snyder, P. R. Jewell and F. J. Lovas, *Astrophys. J.*, 2001, **554**, L81–L85.
- 4 D. T. Halfen, A. J. Apponi, N. Woolf, R. Polt and L. M. Ziurys, *Astrophys. J.*, 2006, **639**, 237–245.
- 5 M. T. Beltrán, R. Cesaroni, R. Neri, C. Codella, R. S. Furuya, L. Testi and L. Olmi, *Astron. Astrophys.*, 2005, **435**, 901–925.
- 6 M. T. Beltrán, C. Codella, S. Viti, R. Neri and R. Cesaroni, *Astrophys. J.*, 2009, **690**, L93.
- 7 M. A. Requena-Torres, J. Martín-Pintado, S. Martín and M. R. Morris, *Astrophys. J.*, 2008, **672**, 352.
- 8 J. K. Jørgensen, C. Favre, S. E. Bisschop, T. L. Bourke, E. F. van Dishoeck and M. Schmalzl, *Astrophys. J.*, 2012, **757**, L4.
- 9 J. L. Bada, *Earth Planet. Sci. Lett.*, 2004, **226**, 1–15.
- 10 D. P. Bartel and P. J. Unrau, *Trends Biochem. Sci.*, 1999, **24**, M9–M13.
- 11 A. Lazcano and S. L. Miller, *Cell*, 1996, **85**, 793–798.
- 12 O. Leslie E, *Crit. Rev. Biochem. Mol. Biol.*, 2004, **39**, 99–123.
- 13 L. E. Orgel, *Trends Biochem. Sci.*, 1998, **23**, 491–495.
- 14 F. H. C. Crick, *J. Mol. Biol.*, 1968, **38**, 367–379.
- 15 L. E. Orgel, *J. Mol. Biol.*, 1968, **38**, 381–393.
- 16 L. E. Orgel, *Cold Spring Harbor Symp. Quant. Biol.*, 1987, **52**, 9–16.
- 17 C. R. Woese, *The genetic code: The molecular basis for genetic expression*, Harper & Row, New York, 1967.
- 18 S. A. Benner, H.-J. Kim and M. A. Carrigan, *Acc. Chem. Res.*, 2012, **45**, 2025–2034.
- 19 M. Yarus, *Origins Life Evol. Biosphere*, 2013, **43**, 19–30.
- 20 M. Levy and S. L. Miller, *Proc. Natl. Acad. Sci. U. S. A.*, 1998, **95**, 7933–7938.
- 21 K. Ruiz-Mirazo, C. Briones and A. de la Escosura, *Chem. Rev.*, 2014, **114**, 285–366.
- 22 R. Breslow, M. Levine and Z.-L. Cheng, *Origins Life Evol. Biosphere*, 2010, **40**, 11–26.
- 23 M. A. Boutlerow, *Comptes rendus hebdomadaires des séances de l'Académie des Sciences.*, 1861, **53**, 145.
- 24 R. Shapiro, *Origins Life Evol. Biosphere*, 1988, **18**, 71–85.
- 25 D. Müller, S. Pitsch, A. Kittaka, E. Wagner, C. E. Wintner, A. Eschenmoser and G. Ohlofsgewidmet, *Helv. Chim. Acta*, 1990, **73**, 1410–1468.
- 26 S. A. Benner, H.-J. Kim, M.-J. Kim and A. Ricardo, *Cold Spring Harbor Perspectives in Biology*, 2010, **2**.
- 27 M. W. Powner, B. Gerland and J. D. Sutherland, *Nature*, 2009, **459**, 239–242.
- 28 C. Harman, J. Kasting and E. Wolf, *Origins Life Evol. Biosphere*, 2013, **43**, 77–98.
- 29 M. E. Jacox and D. E. Milligan, *J. Mol. Spectrosc.*, 1973, **47**, 148–162.
- 30 K. Toriyama and M. Iwasaki, *J. Am. Chem. Soc.*, 1979, **101**, 2516–2523.
- 31 E. P. Kalyazin and G. V. Kovalev, *Khim. Vys. Energ.*, 1978, **12**, 371–373.
- 32 G. A. Baratta, A. C. Castorina, G. Leto, M. E. Palumbo, F. Spinella and G. Strazzulla, *Planet. Space Sci.*, 1994, **42**, 759–766.

- 33 M. H. Moore, R. F. Ferrante and J. A. Nuth III, *Planet. Space Sci.*, 1996, **44**, 927–935.
- 34 M. E. Palumbo, A. C. Castorina and G. Strazzulla, *Astron. Astrophys.*, 1999, **342**, 551–562.
- 35 G. Strazzulla, M. Arena, G. A. Baratta, C. A. Castorina, G. Celi, G. Leto, M. E. Palumbo and F. Spinella, *Adv. Space Res.*, 1995, **16**, 61–71.
- 36 G. Strazzulla, A. C. Castorina and M. E. Palumbo, *Planet. Space Sci.*, 1995, **43**, 1247–1251.
- 37 R. L. Hudson and M. H. Moore, *Icarus*, 2000, **145**, 661–663.
- 38 R. L. Hudson and M. H. Moore, *Radiat. Phys. Chem.*, 1995, **45**, 779–789.
- 39 P. A. Gerakines, W. A. Schutte and P. Ehrenfreund, *Astron. Astrophys.*, 1996, **312**, 289–305.
- 40 C. J. Bennett, S.-H. Chen, B.-J. Sun, A. H. H. Chang and R. I. Kaiser, *Astrophys. J.*, 2007, **660**, 1588.
- 41 C. J. Bennett and R. I. Kaiser, *Astrophys. J.*, 2007, **661**, 899–909.
- 42 P. Modica and M. E. Palumbo, *Astron. Astrophys.*, 2010, **519**, A22.
- 43 P. Modica, M. E. Palumbo and G. Strazzulla, *Planet. Space Sci.*, 2012, **73**, 425–429.
- 44 Y. J. Chen, A. Ciaravella, G. M. M. Caro, C. Cecchi-Pestellini, A. Jimenez-Escobar, K. J. Juang and T. S. Yih, *Astrophys. J.*, 2013, **778**, 162.
- 45 A. L. F. de Barros, A. Domaracka, D. P. P. Andrade, P. Boduch, H. Rothard and E. F. da Silveira, *Mon. Not. R. Astron. Soc.*, 2011, **418**, 1363–1374.
- 46 A. Ciaravella, G. M. Caro, A. J. Escobar, C. Cecchi-Pestellini, S. Giarrusso, M. Barbera and A. Collura, *Astrophys. J.*, 2010, **722**, L45.
- 47 O. S. Heavens, *Optical Properties of Thin Solid Films*, Butterworths Scientific Publications, London, 1955.
- 48 P. Winsemius, F. F. v. Kampen, H. P. Lengkeek and C. G. v. Went, *J. Phys. F: Met. Phys.*, 1976, **6**, 1583.
- 49 A. M. Goodman, *Appl. Opt.*, 1978, **17**, 2779–2787.
- 50 M. S. Westley, G. A. Baratta and R. A. Baragiola, *J. Chem. Phys.*, 1998, **108**, 3321–3326.
- 51 D. M. Hudgins, S. A. Sandford, L. J. Allamandola and A. G. G. M. Tielens, *Astrophys. J. Suppl.*, 1993, **86**, 713–870.
- 52 C. J. Bennett, C. Jamieson, A. M. Mebel and R. I. Kaiser, *Phys. Chem. Chem. Phys.*, 2004, **6**, 735–746.
- 53 A. Wada, N. Mochizuki and K. Hiraoka, *Astrophys. J.*, 2006, **644**, 300.
- 54 R. L. Hudson and M. H. Moore, *J. Geophys. Res.*, 2001, **106**, 33275–33284.
- 55 R. Brunetto, G. Caniglia, G. A. Baratta and M. E. Palumbo, *Astrophys. J.*, 2008, **686**, 1480.
- 56 M. Garozzo, D. Fulvio, Z. Kanuchova, M. E. Palumbo and G. Strazzulla, *Astron. Astrophys.*, 2010, **509**, A67.
- 57 P. Hovington, D. Drouin and R. Gauvin, *Scanning*, 1997, **19**, 1–14.
- 58 R. Luna, M. Á. Satorre, M. Domingo, C. Millán and C. Santonja, *Icarus*, 2012, **221**, 186–191.
- 59 B. D. Teolis, M. J. Loeffler, U. Raut, M. Famá and R. A. Baragiola, *Icarus*, 2007, **190**, 274–279.
- 60 K. I. Öberg, R. T. Garrod, E. F. van Dishoeck and H. Linnartz, *Astron. Astrophys.*, 2009, **504**, 891–913.
- 61 B. M. Jones and R. I. Kaiser, *J. Phys. Chem. Lett.*, 2013, **4**, 1965–1971.

- 62 A. Aspiala, J. Murto and P. Sten, *Chem. Phys.*, 1986, **106**, 399–412.
- 63 J. Ceponkus, W. Chin, M. Chevalier, M. Broquier, A. Limongi and C. Crépin, *J. Chem. Phys.*, 2010, **133**, 094502.
- 64 K. Cai and J. Wang, *J. Phys. Chem. B*, 2009, **113**, 1681–1692.
- 65 R. I. Kaiser, S. Maity and B. M. Jones, *Phys. Chem. Chem. Phys.*, 2014, **16**, 3399–3424.
- 66 J. Lohilahti, T. A. Kainu and V.-M. Horneman, *J. Mol. Spectrosc.*, 2005, **233**, 275–279.
- 67 T.-L. Tso and E. K. C. Lee, *J. Phys. Chem.*, 1984, **88**, 5475–5482.
- 68 J. Lohilahti, T. A. Kainu and V.-M. Horneman, *J. Mol. Spectrosc.*, 2005, **233**, 275–279.
- 69 F. Bell, Q. N. Ruan, A. Golan, P. R. Horn, M. Ahmed, S. R. Leone and M. Head-Gordon, *J. Am. Chem. Soc.*, 2013, **135**, 14229–14239.